

**DEVELOPMENT OF UAV BASED AERIAL
OBSERVATION PLATFORM TO MONITOR MEDIUM
VOLTAGE NETWORKS IN URBAN AREAS**

D.H. Ranasinghe

(159320 A)

Degree Master of Science in Electrical Engineering

Department of Electrical Engineering

University of Moratuwa

Sri Lanka

January 2020

**DEVELOPMENT OF UAV BASED AERIAL
OBSERVATION PLATFORM TO MONITOR MEDIUM
VOLTAGE NETWORKS IN URBAN AREAS**

D.H. Ranasinghe

(159320 A)

Dissertation submitted in partial fulfillment of the requirements for the
Degree Master of Science in Electrical Engineering

Department of Electrical Engineering

University of Moratuwa

Sri Lanka

January 2020

ARTICLE I. Declaration of The Candidate and Supervisor

I declare that this is my own work and this dissertation does not incorporate without acknowledgement any material previously submitted for a Degree or Diploma in any other University or institute of higher learning and to the best of my knowledge and belief it does not contain any material previously published or written by another person except where the acknowledgement is made in the text.

Also, I hereby grant to University of Moratuwa the non-exclusive right to reproduce and distribute my dissertation, in whole or in part in print, electronic or other medium. I retain the right to use this content in whole or part in future works (such as articles or books).

.....

Signature of the candidate

(D.H. Ranasinghe)

.....

Date:

The above candidate has carried out research for the Masters Dissertation under my supervision.

.....

Signature of the supervisor

(Prof. K.T.M. Udayanga Hemapala)

.....

Date:

.....

Signature of the supervisor

(Dr. P.S. Narendra De Silva)

.....

Date:

ARTICLE II. Abstract

Electricity supply outages in urban areas in developing countries like Sri Lanka has a significant impact on the social life as well as the country's economy. Owing to aging of network assets, the frequency of system failures is increasing and therefore, it is a major challenge for utilities to reduce the electricity outages without compromising essential maintenance needs. Therefore, it has become a mandatory requirement to find advanced automated solutions to upgrade traditional procedures in order to reduce the maintenance time.

A deep study about the process flow for planned and un-planned maintenance reveals that inspection is a necessary activity which significantly contributes to the outage time. Apparently, maintenance scheduling also solely depends on inspection results and the quality of results directly influence efficiently of fault clearing or routine maintenance process. Hence, this research was done to develop a solution to reduce inspection time while improving the quality and safety of operation. The scope of the study was identified as the inspection process of short span MV feeders in urban areas and the properties and parameters of this type of feeders were taken to develop the methodology.

As outcome of this research, a quadcopter based aerial observation platform was developed to remotely investigate MV feeders while mitigating the electromagnetic interference. The platform has an imaging unit which transmits images to a ground station and computer based program process images further and identifies defects. In the scope of this research, the MATLAB based algorithm was developed to identify corroded nuts in transformer terminals. The same algorithm can be extended to identify other specific network defects and faults and quadcopter design can be rescaled to operate in a long range as per the desired industrial requirement.

ARTICLE III. Acknowledgement

I would like to express my sincere gratitude to those who were behind me in completing this research project.

I am deeply indebted to my supervisors Dr. Narendra De Silva, Head of Engineering, Lanka Electricity Company and Prof. Udayanga Hemapala, Senior Lecturer, Department of Electrical Engineering, University of Moratuwa for their continuous support and encouragement from starting of this project up to writing this dissertation.

My sincere thanks go to my immediate supervisor, LECO system development manager Mr. S.D.C Gunawardhana and all my colleagues at Lanka Electricity Company Private Limited who helped me in many ways during this period. Further I would like to thank LECO R&D Department for providing the infrastructure for testing and validate algorithms.

Last but not least, I would express my heartiest gratitude and love to my wife, my father, my mother and my brother sister who took a lot of burden and patient, which helped me to complete this work in difficult circumstances.

ARTICLE IV. Table of Contents

ARTICLE I.	Declaration of The Candidate and Supervisor.....	i
ARTICLE II.	Acknowledgement.....	i
ARTICLE III.	Table of Contents	ii
ARTICLE IV.	List of Figures	iv
ARTICLE V.	List of Tables.....	vi
ARTICLE VI.	List of Abbreviations.....	vii
1	INTRODUCTION	8
1.1	Background	9
1.1.1	Sri Lankan Distribution Network.....	9
1.2	Problem Statement	10
1.3	Objectives of Study	10
1.4	Motivation	11
1.5	Methodology	11
2	LITERATURE REVIEW	12
3	DESIGN AND DEVELOPMENT.....	21
3.1	Fault Identification	21
3.1.1	Identification of Reference Points.....	21
3.1.2	Correction of object perspective due to different capturing angle.....	27
3.1.3	Pattern Recognition.....	38
3.1.4	Pattern Clustering.....	39
3.2	Development of the quadcopter	41
3.2.1	Design Inputs	41
3.2.2	Design Calculations	41
3.2.3	Kinematics.....	44
3.2.4	Electrical forces (Motors)	44
3.2.5	Aerodynamic Forces	45
3.2.6	Dynamics of the quadcopter.....	48
3.2.7	Components used in the design.....	49
4	TESTING AND VALIDATION.....	58
4.1	Obtaining close-up, zoom images to study the assembly in details.	58
4.1.1	Insulation Assembly.....	60
4.1.2	DDLO and surge arrester assembly	60
4.1.3	Transformer LV bushing.....	60
4.2	Feeder line surveying	61

4.3	Image patch and defect identification algorithm testing	63
4.4	Quadcopter testing	68
4.4.1	Tuning the parameters	68
4.4.2	Altitude holding function	70
4.4.3	Impact analysis on time and Space requirement for inspection process 71	
4.5	Limitation of the study	71
5	CONCLUSION	73
6	REFERENCES	75

ARTICLE V. List of Figures

Figure 1-1: Maintenance Process Flow Chart.....	9
Figure 2-1 : Front, Left And the Platform View of the Robust Chart.....	12
Figure 2-2: Placement of the Robot Over Obstacle	13
Figure 2-3: State Chart of Robot Pace Over Obstacle	14
Figure 2-4: The Electrical System of Robot	15
Figure 2-5: Line Following Robots.....	17
Figure 2-6: Unmanned Commercial Helicopters	18
Figure 2-7: Fundamental Components Setup.....	19
Figure 3-1 : Model Transformer Used in Algorithm	21
Figure 3-2 : Differentiate reference colour from background.....	22
Figure 3-3 : Image after Filtering Reference Points from the Background	23
Figure 3-4 : Image after Filtering Noise Pixels (High-Pass Filter).....	24
Figure 3-5: Reference points in each quadrant	25
Figure 3-6: Axis of rotation.....	28
Figure 3-7: Rotation over 2-D plane	29
Figure 3-8 : Orientation of the Capturing Angle in the Space	33
Figure 3-9: rotation over Y axis	34
Figure 3-10 : Rotation of the Drone around X-Axis	35
Figure 3-11 : Actual Images W.R.T Rotation over Y Axis	36
Figure 3-12 : 3-D Model for Rotation over Y Axis	37
Figure 3-13 : Projection of 3-D Object on X-Z Plane.....	37
Figure 3-14: Filtered Image after Processing.....	38
Figure 3-15: Circular Hough Transform	40
Figure 3-17 : The Inertial and Body Frames of a Quadcopter	42
Figure 3-18 : Quadcopter Movements	43
Figure 3-19: Vibrating structure gyroscopes.....	50
Figure 3-20 : semiconductor wafer architecture (Left) and the real wafer structure (Right) of an Mem Accelerometer	51
Figure 3-21:Rotor Design	52
Figure 3-22 : Flow diagram of Speed Controlling Mechanism in ESC.....	53

Figure 3-23:General Image of an ESC.....	53
Figure 3-24 : Radio Tx Rx Protocol.....	55
Figure 3-25 : LiPo Battery Rating.....	56
Figure 4-1 : Components Inspected Using the Aerial Imaging Platform - BZ3079 Transformer.....	59
Figure 4-2 : View of the Transformer Assembly from Ground.....	61
Figure 4-3 : Detailed View of the Transformer Assembly from Aerial Imaging	61
Figure 4-4 : Line Surveying - 33kV Feeder Section in UoM	63
Figure 4-5 : Identification of Focus Area to be Processed.....	64
Figure 4-6 : Bit Plane Slicing Algorithm for LV Terminal	65
Figure 4-7 : Before Tuning the PID Parameters in Pitch Axis – Badly Aligned Controlling Signal and Response	69
Figure 4-8 : After Tuning PID Values in Pitch Axis - Controlling Signal and Response is Substantially Overlapped	69
Figure 4-9 : Flight Characteristics of Quadcopter.....	70
Figure 4-10 : Altitude is Remain Constant in the "Altitude Hold" Mode.....	71

ARTICLE VI. List of Tables

Table 1-1: Reliability Indices of LECO 8

Table 2-1: Comparison of Robot Categories 17

Table 3-1 : Coordinates of The Reference Points in Model Transformer..... 27

Table 4-1 : Parameters Used to Identify Corroded Nuts and Bolts 66

Table 4-2 : Summary of Color Patch Detecting Algorithm Testing 67

Table 4-3 : PID values used in Quadcopter 68

Table 4-4 : Impact Analysis on Time and Space Requirement for Inspection Process
..... 71

ARTICLE VII. List of Abbreviations

CAN	Controller Area Network
CCD	Charge-Coupled Device
CEB	Ceylon Electricity Board
DDLO	Drop Down Lift Over
EENS	Expected Energy Not Served
EMI	Electromagnetic Interference
ESC	Electronic Speed Controller
I	Current
kVA	Kilo Volt Ampere
kW	kilo Watt
LECO	Lanka Electricity Company (Pvt.) Ltd.
LV	Low Voltage
MV	Medium Voltage
P	Active Power
R	Resistance
RF	Radio Frequency
RWR	Rolling on Wires Robots
S	Apparent Power
SAIDI	System Average Interruption Duration Index
SAIFI	System Average Interruption Frequency Index
SSE	Sum of Square Error
UAV	Unmanned Aerial Vehicle
V	Voltage
VTOL	Vertical Take Off and Landing
W	Watt

1 INTRODUCTION

Urban infrastructure systems, such as electricity networks, are the backbone of modern societies. In Sri Lankan context, the electricity network plays the most vital role in ensuring the smooth function of all most all the socio-economical systems. Not like in rural areas, where the electricity is used mostly for lightning purposes, in urban areas, the efficiency of most of the functions, starting from ventilating the office premises, up to traffic handling and maintaining security systems, depends on the reliability of the electricity network.

When it comes to maintaining the reliability of the connection supplied to the end customer, healthy operation of the electricity distribution network plays a key role. Reliability data of Lanka Electricity Company (pvt) ltd, one of the power distribution utilities operating in Sri Lankan urban areas, verifies the fact.

Table 1-1: Reliability Indices of LECO

Year	Source Supply Outage Only			LECO Network Outage Only			Total Outages		
	EENS (MWh)	SAIDI (h)	SAIFI (Nos)	EENS (MWh)	SAIDI (h)	SAIFI (Nos)	EENS (MWh)	SAIDI (h)	SAIFI (Nos)
2014	4,371	37.25	81	4,570	22.17	21	8,941	59.42	102
2015	3,587	29.82	66	4,345	20.73	25	7,932	50.55	91
2016	8,587	27.39	66	6,609	40.68	50	15,196	68.07	116
2017	3,807	28.64	66	7,409	41.29	43	11,216	69.93	109
2018	3,687	24.47	47	7,097	31.28	36	10,784	55.75	83

*Source: LECO Statistical Digest 2015,2016,2017,2018

Therefore, the continuous monitoring of the power distribution lines and early identification of faults have become vital requirements. While this consumes a lot of time, effort and man power, UAV provides a practical solution for effective and efficient monitoring of the electricity network. Considering the rapid urbanization trends in Sri Lanka and the popularity in commercial adoption of UAV, electricity utilities will be no exception in commercially utilizing UAV in near future. This research focuses in developing such a UAV based aerial observation platform to monitor medium voltage electricity network in urban areas.

1.1 Background

1.1.1 Sri Lankan Distribution Network

The distribution network of Sri Lanka is almost all overhead, operates in 33 kV and 11 kV medium voltages and 400 V/ 230 V low voltage.

As a regulator in Sri Lankan energy sector, PUCSL has issued five licenses for electricity distribution in Sri Lanka. Out of these five, CEB has four and one license is issued to LECO. PUCSL has provided guidelines and regulations to the utilities on maintaining quality of supply and set goals on reducing energy losses in the network.

The structure of the country's distribution network has not been changed significantly from its formation in early 50s until recent past. The conventional distribution network included only the typical items such as primary substations, MV feeders, distribution Transformers, low voltage feeders, protection and metering mechanisms etc. The power flow was vertically downwards from grid substation to the customer premises through primary substation, MV network, distribution transformer and LV network.

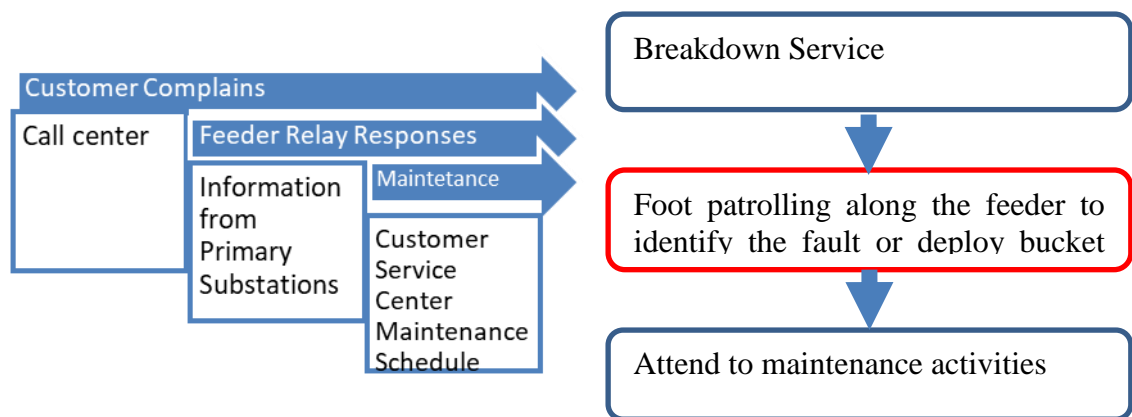


Figure 1-1: Maintenance Process Flow Chart

1.2 Problem Statement

Feeder line inspection is an essential for an electrical distribution utility for operational and maintenance purposes both in planned maintenance and breakdown clearing. In the present situation, this is a manual process with involvement of human intervention. In addition to the related safety issues, inspection process creates more outage time which has an impact on distribution utility performance indices.

In practice, tools used in inspection process with are very few in distribution networks. Generally, inspection process in Sri Lanka is totally done only by skilled technicians and very often, HV line gets de-energized during the process. Usually, during this process, the electricity supply is interrupted minimum for 8 hours for a planned maintenance activity.

To make the process of locating the fault effective and accurate, the observation platform should provide clear and real time statues of the feeder line. Fault identification has to be faster as much as possible to clear the breakdown in a short time. However, depending on the nature of the fault, It is not get detected in the early stages and outage continues until technicians manually check every pole top assemblies in the feeder.

Although commercial drones such as remote controlled quadcopters and planes are available to automate inspections and logistical activities in other industries, it is not often to observe much application in the electricity distribution sector. Substantially high the electromagnetic interference in MV distribution lines has critical impacts on radio and electronic controller units and create challenges in achieving the flying stability in such kind of environment. Therefore, most of the drone project has failed to fulfill economic feasibility to automate inspection process.

1.3 Objectives of Study

Developing a hardware platform to perform aerial inspection in urban medium voltage distribution feeders

- Capability to handle in highly congested areas
- Easy detection of faults
- Reduce human intervention and Improve safety of inspection operation

1.4 Motivation

This research enables to improve the effectiveness of MV line inspection process while improving the human safety as it minimizes the human movement closer to energize equipment.

- Reduce Outage time
- Reduce time to investigate defects
- Provide aerial view and convenient platform to monitor pole top accessories
- Highlight abnormal spots on equipment
- Study the demand elasticity with tariff revisions
- Reduce human intervention and Improve safety of inspection process by providing remote operation

If updated information about the customers and relevant load profiles are available in the databases, above activities can be implemented by the utility.

1.5 Methodology

Major activities of this research can be ordered as follows.

- Literature Survey/ Background Study
 - Investigating the work that has been already carried out under MV line inspection.
 - Identifying the most optimum method for Medium scale urban distribution MV lines
- Developing the platform for aerial imaging and identify faults
- Field testing
- Reporting

2 LITERATURE REVIEW

The overhead MV electrical feeders have become the link between modern industrial and urban community. Maintenance, breakdowns, and services are often in service for these power lines. Commonly used current inspection methods are People online method, telescope, and using a helicopter for inspections. As these methods take time and effort a lot, different innovations have been carried out in order to overcome those difficulties over the tower due to the complex of the structure and control.

A mobile robot design has been created and developed for overhead power line inspection and a controlling method to avoid obstacles which is composed of three suspended arms along with the 03 rolling wheel machine which is coordinated with each other, 03 nodes CAN bus-system and use of a camera system which can transmit images with wireless CCD.

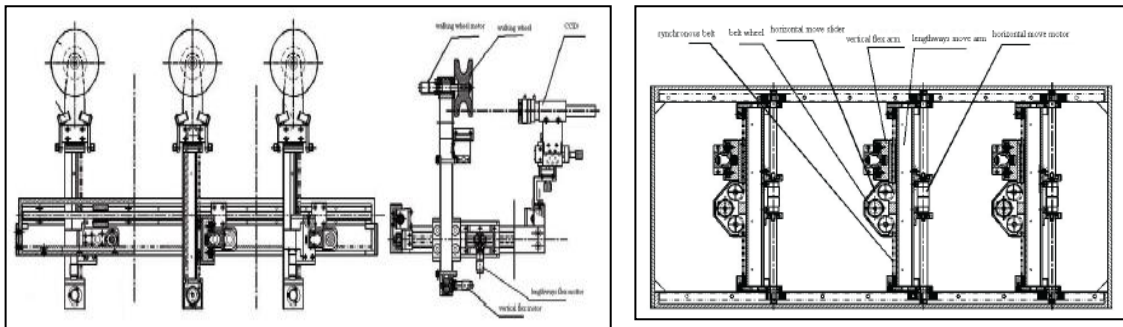


Figure 2-1 : Front, Left And the Platform View of the Robust Chart

The walking module structure over an obstacle has been designed in three axes with the idea of modulation and is has 3 arms which are connected to moving in three hanging axles. This is consisting of moving structure, horizontal and vertical flex arms, and horizontal moving structure. The walking structure consist of movable wheel, driving motor with hinges and fix-up bracket.

Control system design and implementation has been carried out on three-phase bare conductor lines and grounding cables on tower. In this design 3 suspension arms

have been fixed in order to fasten the frame by the steering gear. The upright flexible arm along with the horizontal flex arm are fixed perpendicularly. (Zhang Liyan, 2011)

In this design, vertical arms are used to move the machines break away or move up along the conductor cables while the horizontal flexible arm is used to connect vertical arms and move machine along the plane. The plane moving body has pinion-and-rack steering gear and guide, driving upright and horizontal flexes arms by rolling bearing. (Zhang Liyan, 2011) This makes easy for the three flex arms to move separately along X, Y and Z directions. Therefore, the robot can move over obstacles along the conductor pathway.

Optical Sensors and Touch sensors that are mounted on the right and the left of each flex arms help in detecting obstacles. These sensors detect obstacles at a 10cm distance, although the driving motor which is connected to walking wheel slows down to stop when the touch sensors to detect obstacles in the front.

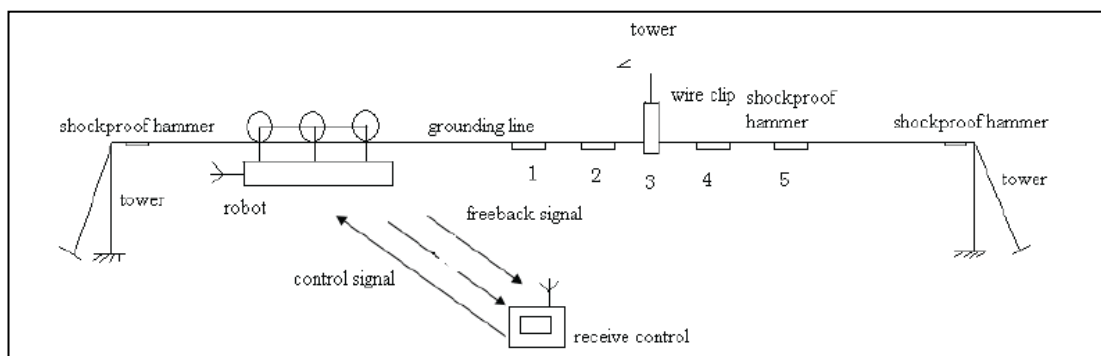


Figure 2-2: Placement of the Robot Over Obstacle

In design and the implementation stage, the object has been selected is a suspension tower, not a strain tower, which consists of a three-phase electrical line and grounding wires cable on the tower. As described in figure 2, the obstacles on the electrical lines are split clapboards with intervals of 10m to 20m. The obstacle near the electrical tower is wire clip hanging on suspension insulator string, and wire clip and vibration damper are the obstacle seen in the grounding wire.

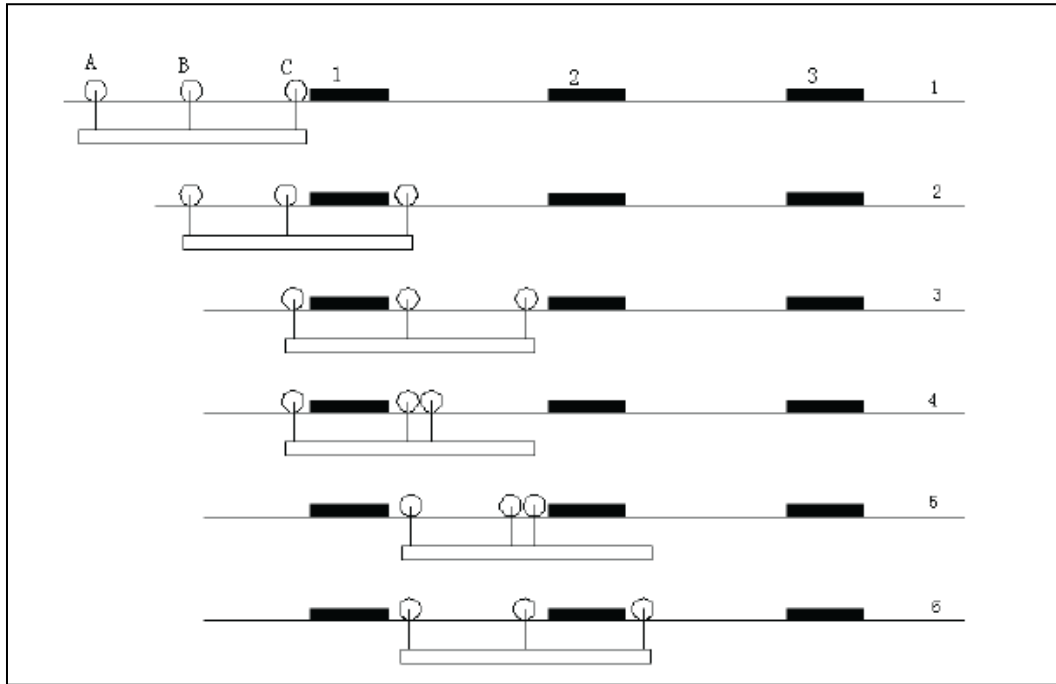


Figure 2-3: State Chart of Robot Pace Over Obstacle

As implemented here, the robot can walkover these obstacles which is indicated with wire clip 3 and vibration dampers (1, 2, 4 and 5) where suspension tower with 220 ~500kV.

As shown in above figure, the robot is moving where it can move along the suspension line which contains three obstacles with the same size. This robot takes the size of lager two obstacles. The intervals between the obstacles can accommodate two moving wheels of the robot.

The system electric design system has modules in both online and down- line. Where online module consists of CCD optic imaging and wireless image emission along with 3 nodes wireless controlling and a battery for the CAN bus. The down-line module has of a wireless receiving unit and an image processing section, battery unit and a controlling system.

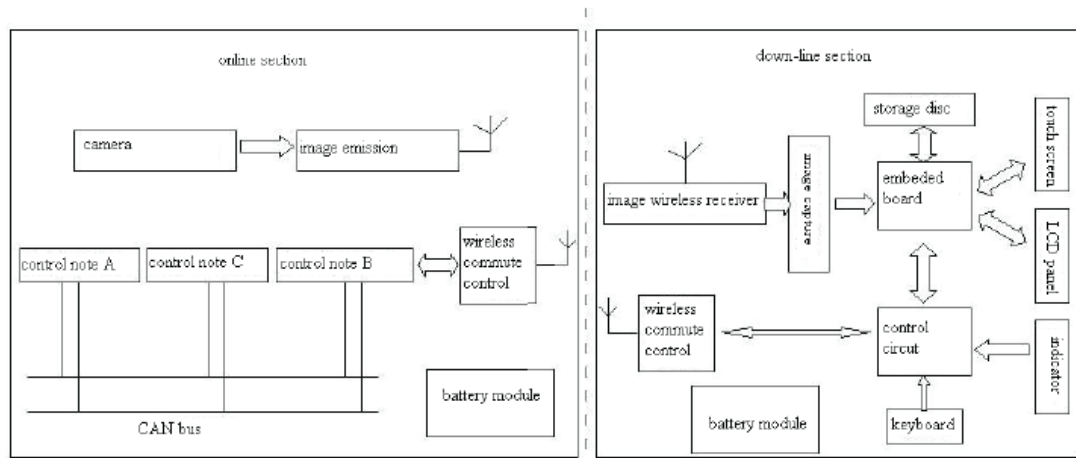


Figure 2-4: The Electrical System of Robot

Broken strands, bulk shares, surface corrosions and conductor splits can be detected from the CCD camera which has been used to identify those surface geometric failures of conductors and optical cable. The images were transmitted online and received and processed by receiving ground station control machine. This system replaces the current inspection method and detecting method of using telescope by manpower along a wire.

This robot designed for overhead power line inspection, can save a lot of labor and increases the detection efficiency and accuracy. Even though this is a successful method to walk through the suspended line and use of optical sensors and touch sensors to detect obstacles, the MV distribution line design of LECO, in the current context, has post insulators with cross arms. Therefore, the development of this methodology, the robot structure will be bulky and heavy for these line designs.

The lines are always operated at an extreme level and there are no reserves or any other termination process to compensate breakdowns. Protective maintenance is therefore of extreme importance. High-voltage networks usually running across suburban environments, forest, mountains, and coastal areas are often exposed for a long period to vigorous working conditions such as thermal excursions, heavy rain, and wind-induced vibration, heavy temperatures, etc. these extreme climatic events vulnerable for corrosion and other failures induce fatigue ruptures which reduces the life span of the lines and it gives high losses to the company.

Addressing to these problems, presenting the state of art of the most important current projects running in different contexts, concerning the two main categories of robots offering a solution of automation. There are, (Pagnano. A, 2013)

- Vertical take- off and landing (VTOL)
- Unmanned aerial vehicles (UVAs)
- Rolling on wires robots (RWR)

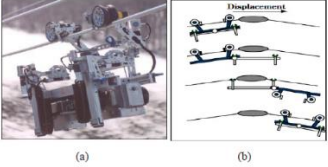
This research creates a simple roadmap that can guide researchers and industries in the implementation of a live line power line inspection. This is based on a completely autonomous mobile platform that consists of the following.


- Compatible payload
- Power line data management system

Which includes specific tool for image and signal data processing to automatically detect defects and other abnormal conditions. This is to create a reliable electrical power the supply system and at the same time to reduce the cost and time.

The main categories of Power line inspection robots, such as vertical takeoff and landing (VTOL) unmanned aerial vehicles (UAVs) and rolling on wires robots (RWR) consumed different robotic technologies and operating systems which have been developed through time. Advantage and disadvantages of these categories are as follows: (Pagnano. A, 2013)

Table 2-1: Comparison of Robot Categories

Method	Advantages	Disadvantageous
<p>Rolling on wire robots (Line following robots/ Line scouts)</p>  <p>Fig. 2. (a) LaneScout Technology, (b) obstacle-clearing sequence [10]</p> <p>Figure 2-5: Line Following Robots</p>	<ul style="list-style-type: none"> • Operate very close to conductors and therefore can detect conductor faults • Can cross damper spheres, Corona Rings, Double insulator rings, etc. • Usually carry weights up to 100kg • not limited to a specific distance between adjacent obstacles 	<ul style="list-style-type: none"> • Crossing dead end assemblies and post insulators are not considered • Slow operation due to significant time taken for avoid obstacle • Radial imaging is not possible in order to inspect line assemblies • High installation time on cables prior operation (approximately 2 hours) • Not good for short span lines on post insulators
<p>VTOL heavy weight UAVs (Unman commercial Helicopters)</p>	<ul style="list-style-type: none"> • Imaging is possible in wide operational range • Fuel operated UAVs has high flight time • Micro turbine powered UAVs can carry around 12kgs • Can carry specified sensors such as corona probes, HD cameras and 	<ul style="list-style-type: none"> • High cost of operation • Need skilled pilot to operate the UAV • Cannot get closer to power line accessories.

 <p>Fig. 7. (a) commercial radio controlled helicopter [22]; (b) T21 [23]</p> <p>Figure 2-6: Unmanned Commercial Helicopters</p>	<p>Thermal Images as both power and weight can be tolerated</p>	
<p>VTOL light weight UAVs (Small scale multi-rotors)</p>	<ul style="list-style-type: none"> • Low cost of operation • Image processing and feature tracking is possible • High mobility • Easy to deploy 	<ul style="list-style-type: none"> • Low payload (< 2kg) • Flight time constrains – Power source issues • Cannot get closer to power line accessories. • EMI on electronic and RF communication

In the above assignment, the main fundamental was to develop a data management system including specific tool for image and signal data processing to automatically detect defects or abnormal conditions. These automated systems are capable to elaborate all the data stored gives an essential additional value to optimize the advantages making further difference with respect to the traditional inspection methods. (Pagnano. A, 2013)

Even though these technologies developed to maintain a better power supply system, in the current context, the LECO MV distribution line designs have short spans about 35m to 40m and conductors are placed on post insulators and cost for the above operations will be high. Addressing these problems, a small scale multirotor (Quadcopter) will be sufficient as the aerial platform in designing.

These multirotor project dedicated to completely autonomous inspection of power line, are still an emerging technology which needs further improvements for better

concrete results. Projects which are considered in particular specific constraints for a completely autonomous live-line inspection can be seen in different areas.

Visual surveying for power line tracking, obstacle detection and avoidance (especially during a crash in live line, this is important for a reliable autonomous inspection system), Robust control algorithms for flight dynamics, ensuring a very high stability and positioning capability for close and precise inspections in particular in case of adverse weather conditions like strong lateral wind and rain. (Pagnano. A, 2013) Thus automated systems make a further difference with the traditional system adding more advantages which is cable to elaborate all the data stored gives a vital additional value.

A theoretical development and a study has been carried out on takeoff constrain thrust equation for a drone or a multirotor and validate the results with web simulation. These theory equations are useful for the drone application in the extra features design during the fly which is consist of a camera, thermal sensor, wireless sensor and other sensors application. (Shen Huang.C, 2017)

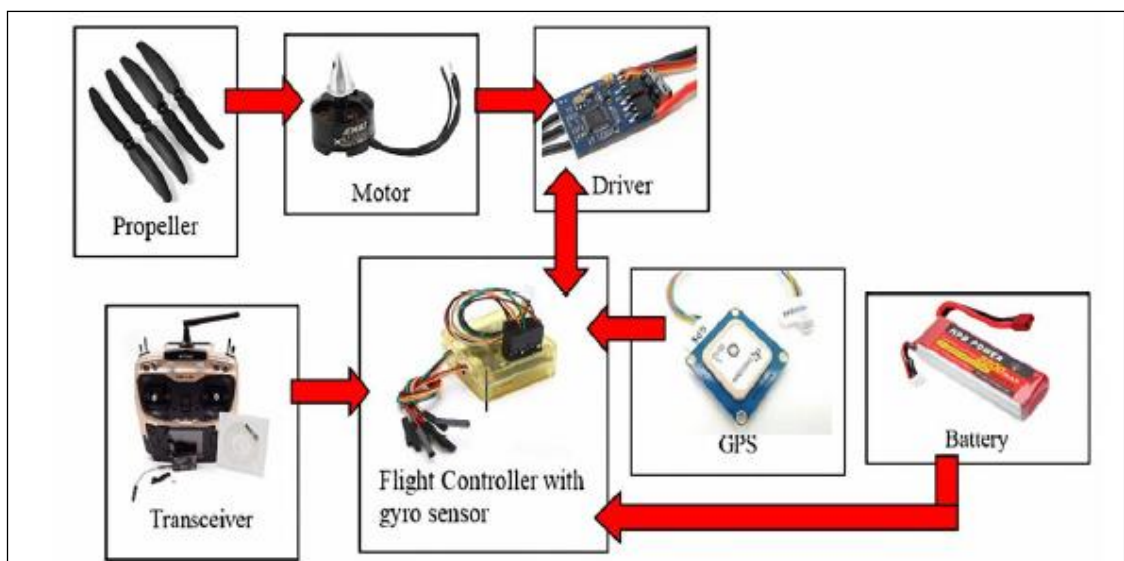


Figure 2-7: Fundamental Components Setup

A drone consists of a pair of diagonal propeller which rotate clockwise while another pair will rotate counter-clockwise. This movement helps in control the direction and achieve the movement of the drone. A quadcopter requires a Gyroscope, Global Positioning System (GPS), Flight controller, transceiver, motor speed driver, flight

controller, Lipo-battery, brushless DC motor, propeller and quadcopter airframe. The fundamental components of a drone set up can be seen in above figure.

3 DESIGN AND DEVELOPMENT

The design component of the research was cascaded in to two section in order to identify abnormalities in the network components and development of a quadcopter drone, respectively.

3.1 Fault Identification

3.1.1 Identification of Reference Points

It is required to identify the particular area for further processing with reference to the predetermined demarcations of an equipment. In order to develop this algorithm, a model transformer is selected.

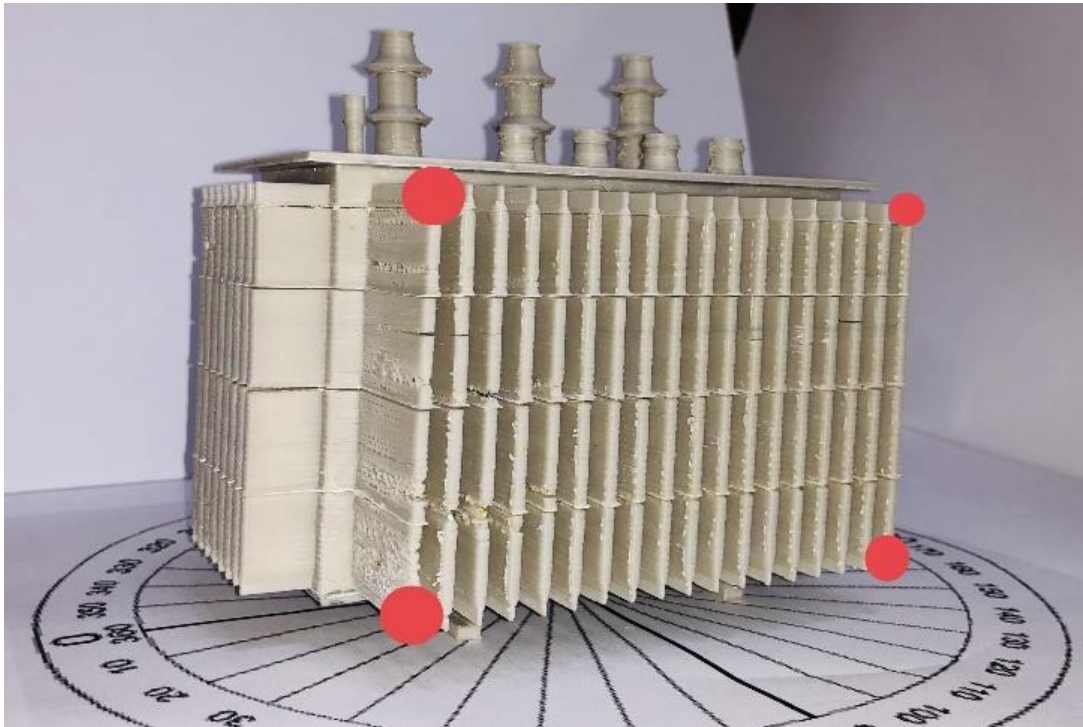


Figure 3-1 : Model Transformer Used in Algorithm

The reference points are considered as red points (RGB : 273,70,75) as of the used model. In practical conditions, predetermined demarcations in the transformer can be considered as the references.

1. The image matrices are cascaded to three 2-D matrices for each color properties. The corresponding value is subtracted from each color plane. When the 2-D matrices are combined together to regenerate the image again, the intensity level of reference points becomes close to zero and therefore these points become black spots.

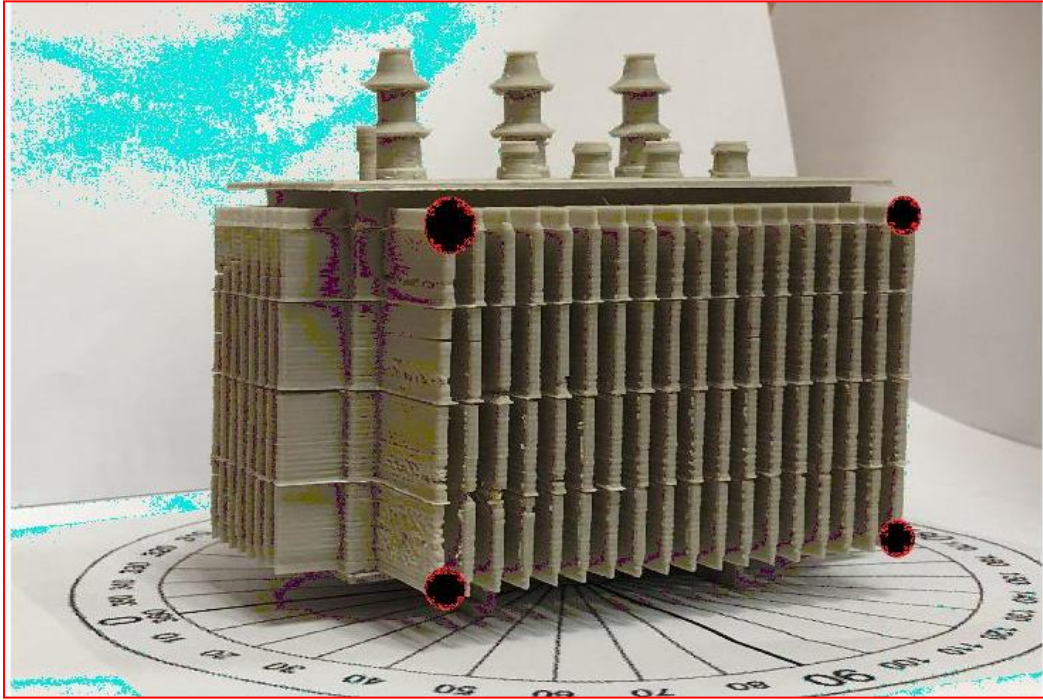


Figure 3-2 : Differentiate reference colour from background

1.b) identifying location of referenced points

The gray scale image of the previous image was obtained by adding intensities of all color plains together.

$$g(x, y) = \sum_{x=1}^n \sum_{y=1}^m (RedPlan(x, y) + GreenPlan(x, y) + BluePlan(x, y))$$

As the intensity of the reference points in all color plains are close to zero, it will appear as black patches in the grayscale image.

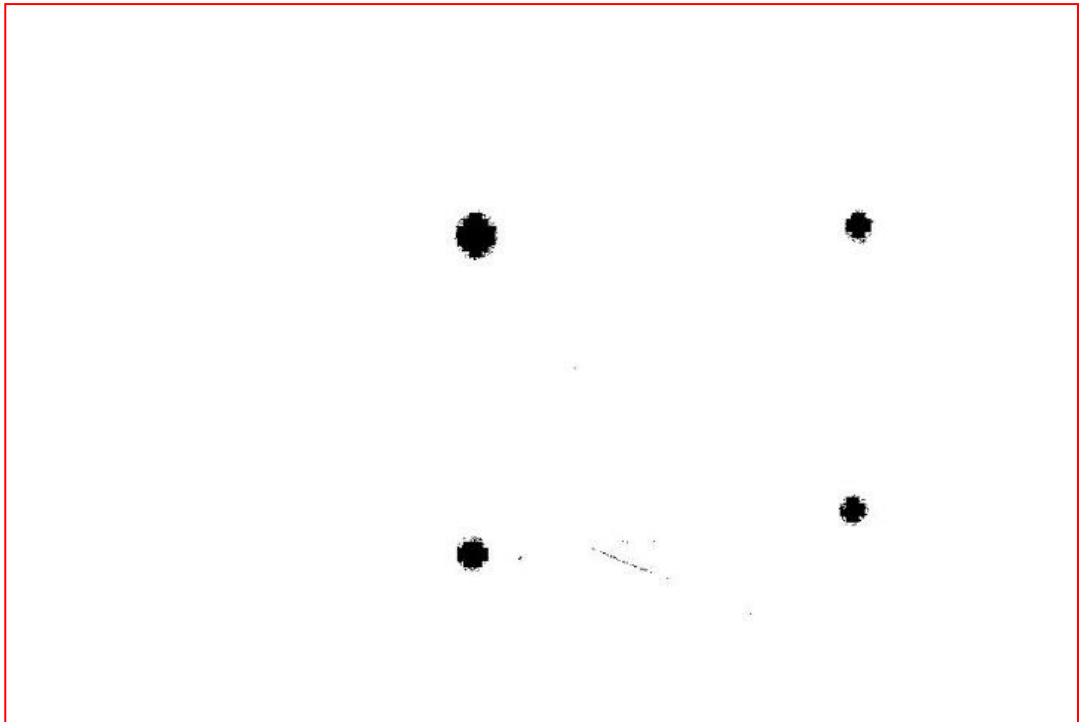


Figure 3-3 : Image after Filtering Reference Points from the Background

2. Removing the noise in the grayscale image

During the image transformation process, some registers related to pixels' values overflows and becomes empty due to matrices operations. This become a noise in the image and it could negatively impact the accuracy of the calculations. These Impulse noise, shot noise, spike noise and drop out noise can be categorized as salt (white pixels) and pepper (black pixels) which usually create bigger impact comparing to other type of noises.

There are many methods to eliminate this salt and paper noises and depending on requirement of high speed image processing, the Median filter is used.

The median filter replaces the pixel value with the median value of the adjacent pixels. This function is usually a 3x3 kernel which moves from first to last pixels

while eliminating the noises. The kernel operator(T[]) could be any size and the elements could be weighted forward or backward if necessary.

Kernel

$$T[] = \begin{array}{|c|c|c|} \hline 1/9 & 1/9 & 1/9 \\ \hline 1/9 & 1/9 & 1/9 \\ \hline 1/9 & 1/9 & 1/9 \\ \hline \end{array}$$

Kernel Operation

Image Matrix (V)

1	5	4
2	100	12
11	3	16



T[V]

	17	

Therefore, low frequency pixels in the image is eliminated by moving the kernel through the grayscale image.

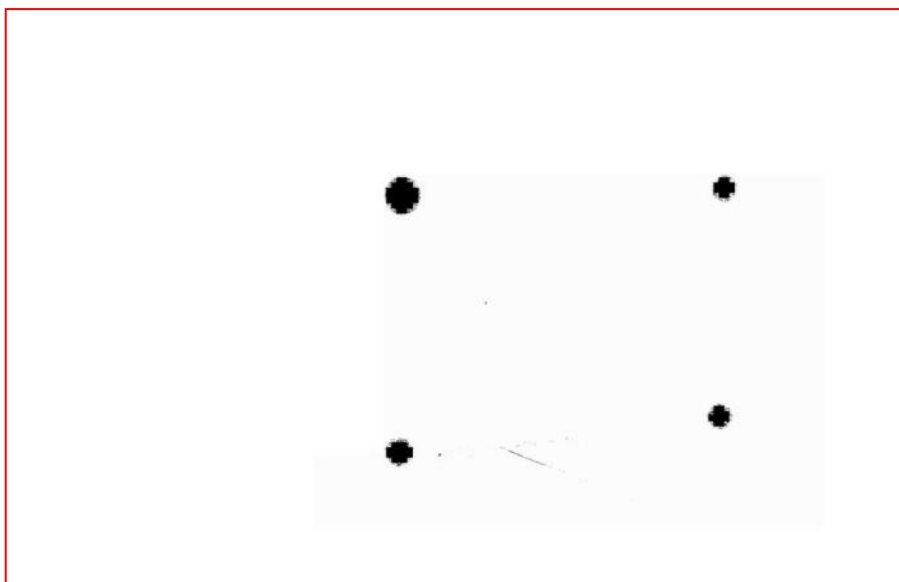


Figure 3-4 : Image after Filtering Noise Pixels (High-Pass Filter)

$$\begin{aligned}
&gAverage(x, y) \\
&= \sum_{x=1}^n \sum_{y=1}^n ((g(x, y) + g(x + 1, y + 1) + g(x, y + 1) \\
&\quad + g(x - 1, y + 1) + g(x + 1, y) + g(x, y) + g(x - 1, y) \\
&\quad + g(x + 1, y - 1) + g(x, y - 1) + g(x - 1, y - 1))/9
\end{aligned}$$

Depending on the required level of accuracy, this operation can be done several times using the same kernel or different kernels. Owing to the nature of the grayscale images used for the project, the same kernel was used in repeat operations for five times.

$$\begin{aligned}
&gAverage(x, y) \\
&= \sum_{R=1}^5 \sum_{x=1}^n \sum_{y=1}^n ((g(x, y) + g(x + 1, y + 1) + g(x, y + 1) \\
&\quad + g(x - 1, y + 1) + g(x + 1, y) + g(x, y) + g(x - 1, y) \\
&\quad + g(x + 1, y - 1) + g(x, y - 1) + g(x - 1, y - 1))/9
\end{aligned}$$

As the image is clearly separated with black and white pixels, the location of the reference points can be obtained identifying the gravity of the black pixels in each section of image. The inverses of the picture gives the exact location of the most significant pixels and location of these significant pixels are calculated.

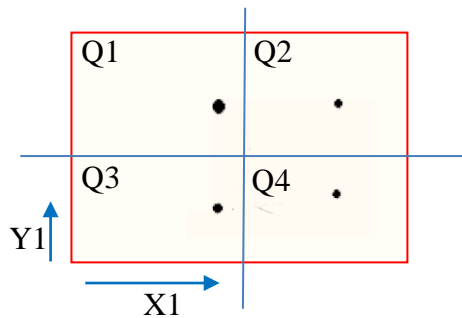


Figure 3-5: Reference points in each quadrant

Generally, the object is captured covering more than 80% of the background, reference points of the object are placed in each quadrant of the image as shown in

above figure. Therefore, coordinates of reference points in each quadrant is calculated.

Image matrix = $g(m, n)$

$$\left(\begin{array}{cc} Q1 = g[0:\frac{m}{2}, \frac{n}{2}:n] & Q2 = g[\frac{m}{2}:m, \frac{n}{2}:n] \\ Q3 = g[0:\frac{m}{2}, 0:\frac{n}{2}] & Q4 = g[\frac{m}{2}:m, 0:\frac{n}{2}] \end{array} \right)$$

inverse image matrix ($\hat{g}(m, n)$) = $255 - g(m, n)$

Coordinates of the reference point in Q3,

$$X_1 = \frac{\sum_{j=1}^{n/2} ((\sum_{i=1}^{m/2} \hat{g}(i, j)) \times j)}{\sum_{j=1}^{n/2} \sum_{i=1}^{m/2} \hat{g}(i, j)}$$

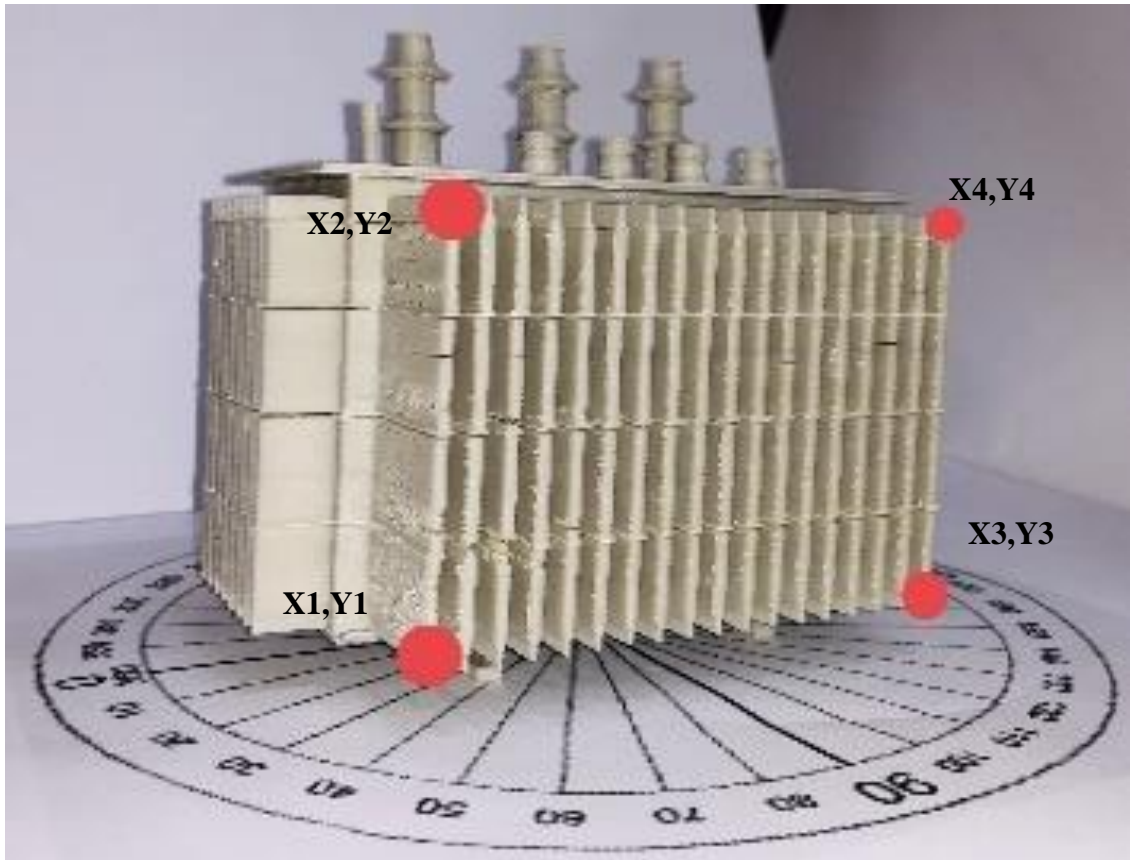
Likewise, Y1 also can be expressed as,

$$Y_1 = \frac{\sum_{i=1}^{m/2} ((\sum_{j=1}^{n/2} \hat{g}(i, j)) \times i)}{\sum_{j=1}^{n/2} \sum_{i=1}^{m/2} \hat{g}(i, j)}$$

Therefore, the reference points in the model transformer is obtained as tabulated below. This coordinates are calculated in each frame and algorithm execution speed is directly impact on the frame rate for image capturing.

Table 3-1 : Coordinates of The Reference Points in Model Transformer

Reference points	X - coordinate	Y - coordinate
(x1,y1)	488	928
(x2,y2)	482	1888
(x3,y3)	1162	1881
(x4,y4)	1225	925



3.1.2 Correction of object perspective due to different capturing angle.

When processing images to identify the faults, it is important to isolate the relevant object from the background which is captured in the frame. Although the shape and the size of this object is known, it becomes difficult to filter this object out of the image background if it is oriented in a different angle. Owing to the nature of the drone imaging, this angle of orientation changes from image to image. The practical difficulties in the field such as vegetation obstacles, flight protocols and safety

clearance regulations, it is not possible to always capture images of the objects in the same favorable direction. But orientation has to be identical in order to analyze the comparison with reference images.

3.1.2.1 Approach

The capturing angle of the image can be considered as a rotated image of the 3-D object of the equipment. As the reference points of the equipment is known, coordinates of the original equipment boundaries of the front elevation of the image can be obtained using 3-D coordinate transformation method.

In general, the conversion effect on a 2D or 3D object doesn't change the shape or the size of the object but varies from a simple change in location and to a uniform change in scale. Ultimately, changes in Shape and size of varying degrees of non-linearity. Therefore, Helmert transformation is used to obtain the coordinates of corrected reference points. (DEAKIN, 1998).

Helmert transformation

$$\begin{bmatrix} x' \\ y' \\ z' \end{bmatrix} = \lambda R_{K\phi\omega} \begin{bmatrix} X \\ Y \\ Z \end{bmatrix} + \begin{bmatrix} R \\ P \\ Q \end{bmatrix}$$

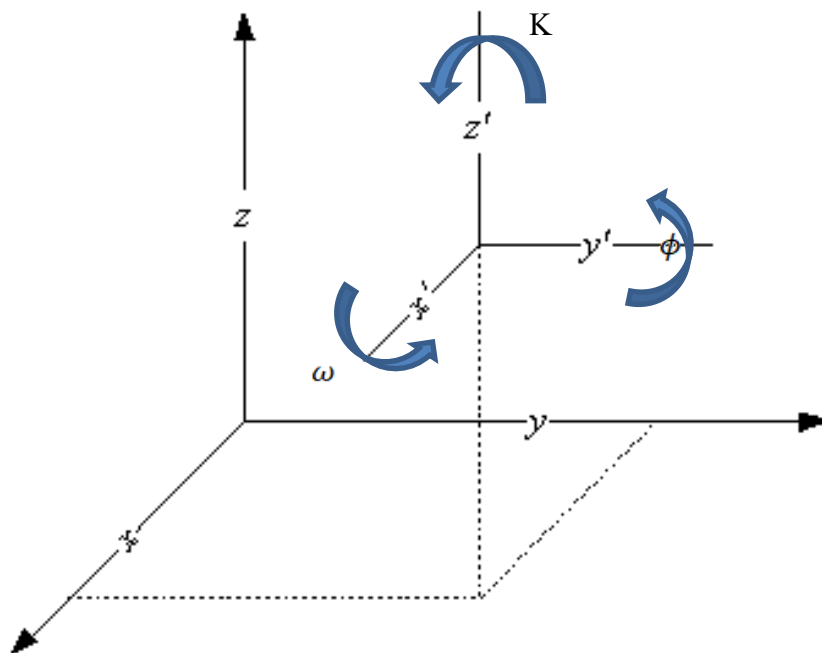


Figure 3-6: Axis of rotation

$R_{K\phi\omega}$ is a rotation matrix (the product of rotations ω, ϕ , and K about the X, Y and Z axes in turn).

Considering the nature of Matrix $R_{K\phi\omega}$, it is not possible to solve directly for the each rotations of K, ϕ and ω axis. Therefore, first the equation is derived for a transformation between two planes.

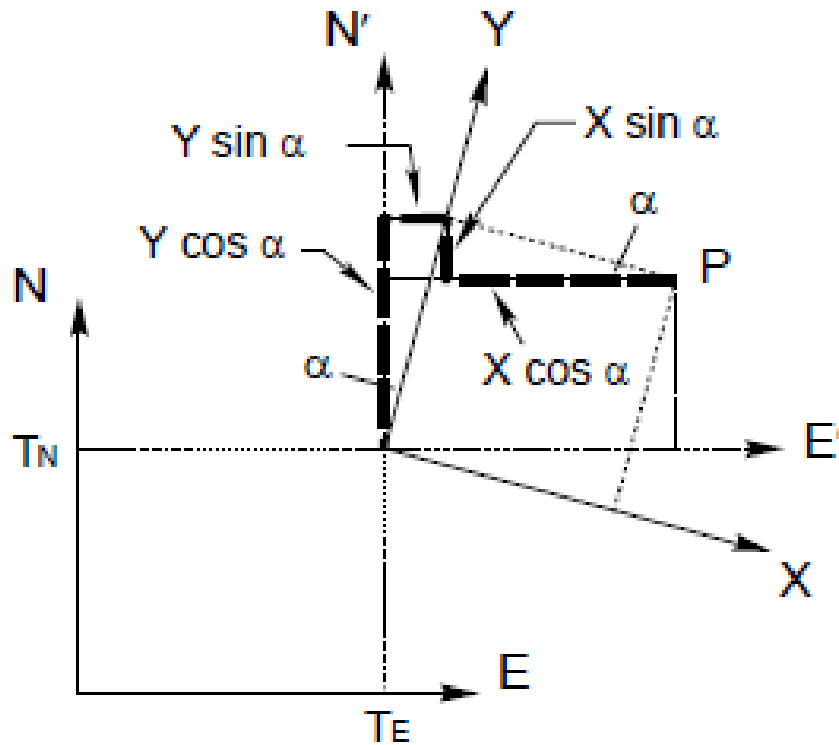


Figure 3-7: Rotation over 2-D plane

Gaussian complex expression the transformation from two plans can be detonated by

$$y + ix = f(\chi + i\omega)$$

Here, i is a complex number and $f(\chi + i\omega)$ is analytic function and parameter X and Y are the dimensions of the object. If the function is analytic, it is a necessary condition to satisfy the Cauchy-Reimann equation. Then it is also considered as a polynomial function and therefore, the function can be represented as;

$$y' + ix' = \sum_{k=0}^n (a_k + ib_k)(Y + iX)^k$$

for k=1 condition equating real and imaginary parts,

$$y' = a_0 + a_1Y - b_1X$$

$$x' = b_0 + a_1X + b_1Y$$

This equation is represented by a matrix

$$\begin{bmatrix} y' \\ x' \end{bmatrix} = \begin{bmatrix} a_1 & -b_1 \\ b_1 & a_1 \end{bmatrix} \begin{bmatrix} Y \\ X \end{bmatrix} + \begin{bmatrix} b_0 \\ a_0 \end{bmatrix}$$

a_0 and b_0 is considered as the transformation of the origin, a_1 and b_1 can be considered as function of scale factor and rotation angle between coordinate axes.

$$a_1 = \lambda \cos \alpha$$

$$b_1 = \lambda \sin \alpha$$

Therefore, transformation in 2-D can be represented by scaling factor and rotational angle as follows,

$$\begin{bmatrix} y' \\ x' \end{bmatrix} = \lambda \begin{bmatrix} \cos \alpha & -\sin \alpha \\ \sin \alpha & \cos \alpha \end{bmatrix} \begin{bmatrix} Y \\ X \end{bmatrix} + \begin{bmatrix} b_0 \\ a_0 \end{bmatrix}$$

The rotational matrix ($R\alpha$) for 2-D plan,

$$R_\alpha = \begin{bmatrix} \cos \alpha & -\sin \alpha \\ \sin \alpha & \cos \alpha \end{bmatrix}$$

Transformation in 3-D axis

A 3-D transformation can be considered as three subsequent transformations between 2-D plans.

Step 1

Rotation of ω about X-axis changes Y and Z to y' and z' with X axis to x' . coordinates of the new system will be given by,

$$\begin{bmatrix} x' \\ y' \\ z' \end{bmatrix} = \underbrace{\begin{bmatrix} 1 & 0 & 0 \\ 0 & \cos \omega & \sin \omega \\ 0 & -\sin \omega & \cos \omega \end{bmatrix}}_{R_\omega} \begin{bmatrix} X \\ Y \\ Z \end{bmatrix}$$

Step 2

Transformation of x', y', z' system to x'', y'', z'' system with the rotation of ϕ about new y' axis.

$$\begin{bmatrix} x'' \\ y'' \\ z'' \end{bmatrix} = \underbrace{\begin{bmatrix} \cos \phi & 0 & -\sin \phi \\ 0 & 1 & 0 \\ \sin \phi & 0 & \cos \phi \end{bmatrix}}_{R_\phi} \begin{bmatrix} x' \\ y' \\ z' \end{bmatrix}$$

Step 3

Transformation of x'', y'', z'' system to x''', y''', z''' system with the rotation of K about new z'' axis.

$$\begin{bmatrix} x''' \\ y''' \\ z''' \end{bmatrix} = \underbrace{\begin{bmatrix} \cos K & \sin K & 0 \\ -\sin K & \cos K & 0 \\ \sin \phi & 0 & 1 \end{bmatrix}}_{R_K} \begin{bmatrix} x'' \\ y'' \\ z'' \end{bmatrix}$$

Therefore 3-D rotational matrix can be obtained by multiplying co-efficient matrices of above three steps.

$$\begin{bmatrix} x''' \\ y''' \\ z''' \end{bmatrix} = R_\omega R_\phi R_K \begin{bmatrix} X \\ Y \\ Z \end{bmatrix}$$

Rotational matrix for 3-D transformation,

$$R_{\omega\phi K} = R_{\omega}R_{\phi}R_K = \begin{bmatrix} C_{\phi}C_K & C_{\omega}S_K + S_{\omega}S_{\phi}C_K & S_{\omega}S_K - C_{\omega}S_{\phi}C_K \\ -C_{\phi}S_K & C_{\omega}C_K - S_{\omega}S_{\phi}C_K & S_{\omega}C_K + C_{\omega}S_{\phi}S_K \\ S_{\phi} & -S_{\omega}C_{\phi} & C_{\omega}C_{\phi} \end{bmatrix}$$

Obtaining the parameters to transform images

Quadcopter is designed to always operate in a leveled position to minimize the rolling angle due to the nature of its flight dynamics. Therefore, the rotation around z axis is negligible and K can be considered as zero. Rotation over x axis (ω) depends on the drone flying height and type of the observation and detail requirements. With respect to below image, if the drone is used to monitor top part of assemblies such as cable preforms, top section of insulators, it is required to increase camera angle and keep the drone at higher position (ω_B). When it is used to monitor lower elements such as transformer components and cross-arm fittings, the camera angle will be low (ω_A), and the flying height will be kept at lower level.

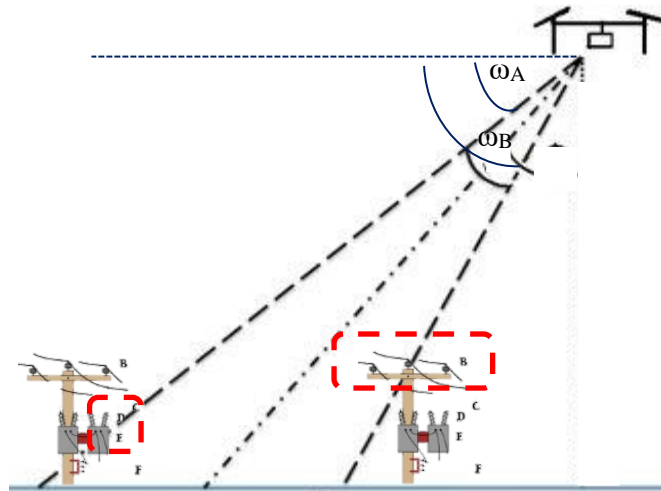


Figure 3-8 : Orientation of the Capturing Angle in the Space

In this case study, the drone will be used to monitor transformer components and it will be kept at the same level as the transformer while keeping the camera at horizontal position. Therefore, the rotation over X axis (ω) is very minimal and can be neglected.

Owing to the restrictions in flying regulations and other obstacles, it is almost impossible to keep the drone straight to the object while avoiding roads and pedestrian ways in urban areas. Hence, images were taken at angle and the object has rotation over Y axis as ϕ .

3.1.2.2 Obtaining the Correct Rotational Angle over Y Axis (Φ) to Correct the Given Image.

As described in the section, designing of the platform, the rotational angles of three axis of the drone is continuously monitored to perform the flight. Yaw angle is measured by an accurate, high speed compass in order to obtain the drone orientation with respect to the North Pole. This real time data is received to the ground station via the telemetry unit and this can be used to calculate the image rotational angle over Y axis.

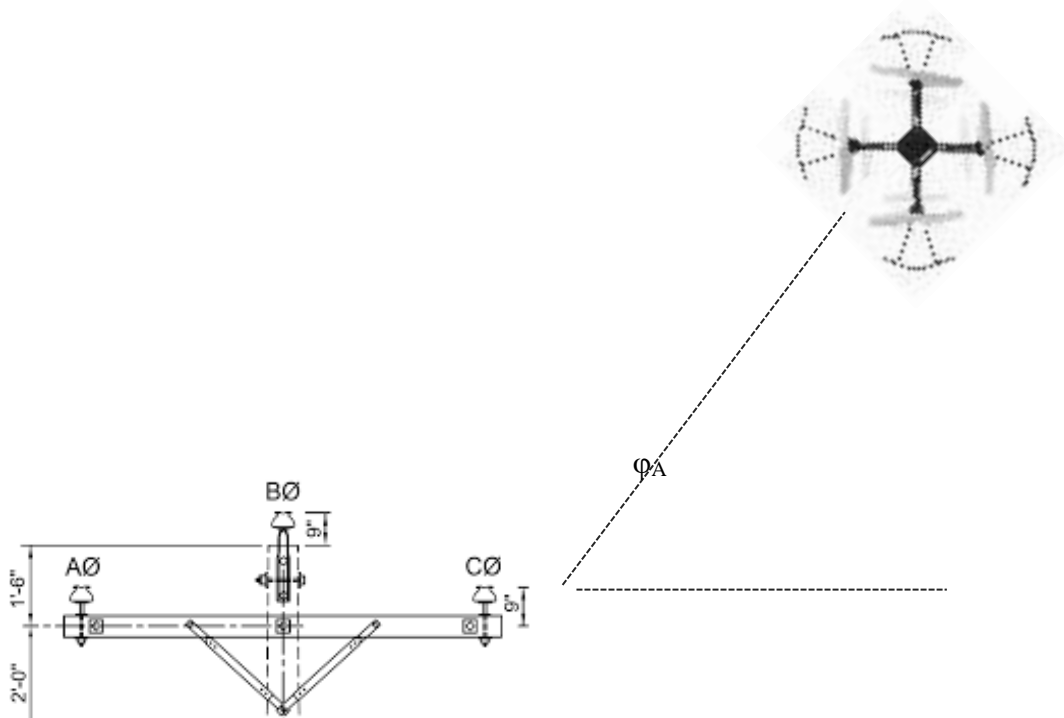


Figure 3-9: rotation over Y axis

During the initial take off, drone is kept in the same orientation as the object and therefore, any rotation in Y axis during the flight, is represented by the difference in the yaw angle. Usually the drone and camera is started at the same time, the time domain is same in the captured images and data received from the drone. Hence, the rotation in Y axis for an Image which is taken at time “t”, can be obtained as ϕ_A using below graph.

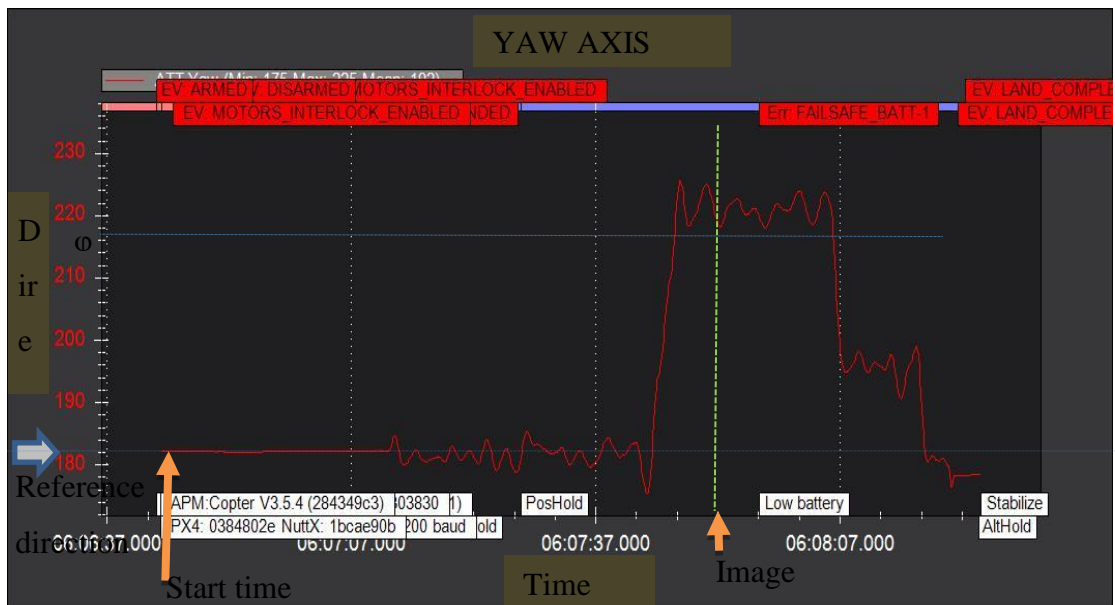
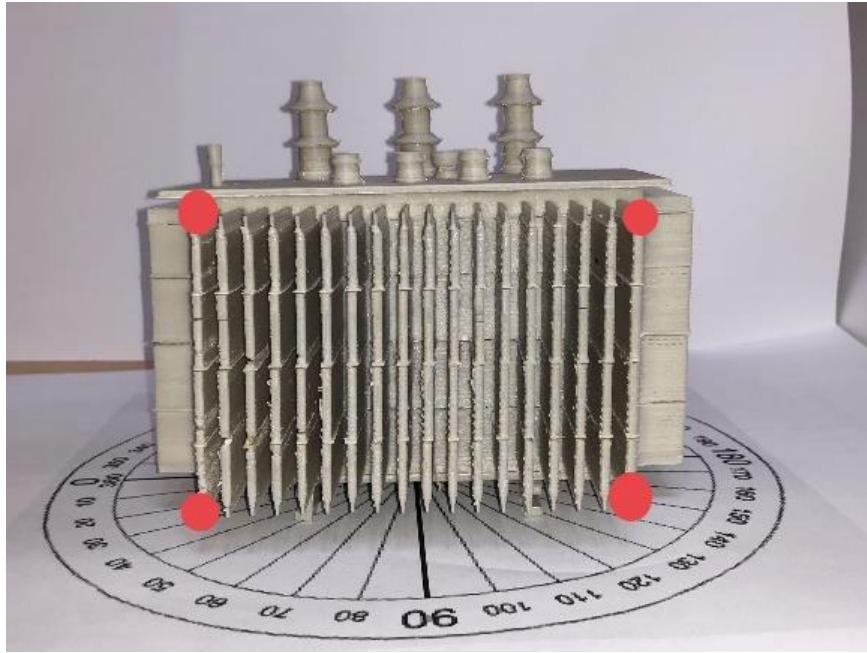


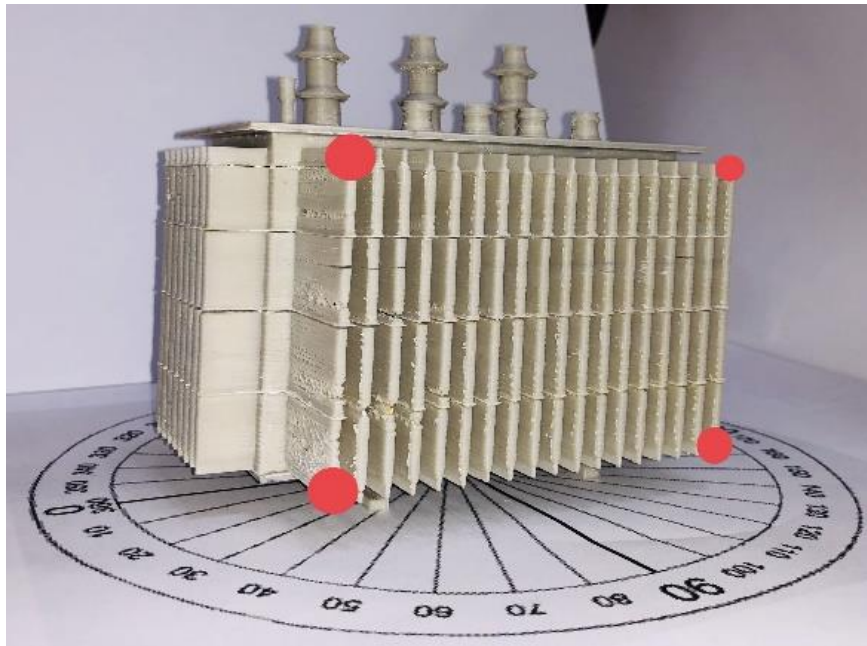
Figure 3-10 : Rotation of the Drone around X-Axis

3.1.2.3 Filtering object from image background

As the location and the size of the object is known from Methodology 01, it is possible to create a 3-D point cloud for the same object. The closets reference point (x_1, y_1) is considered as the origin of 3-D point cloud object and the dimensions is taken as proportional to the height of the object in the captured image. $(x_1, y_1$ and $x_2, y_2)$



Rotation over y axis = 0°



Rotation over y axis = 30°

Figure 3-11 : Actual Images W.R.T Rotation over Y Axis

1. Base image for algorithm

3-D point cloud for object

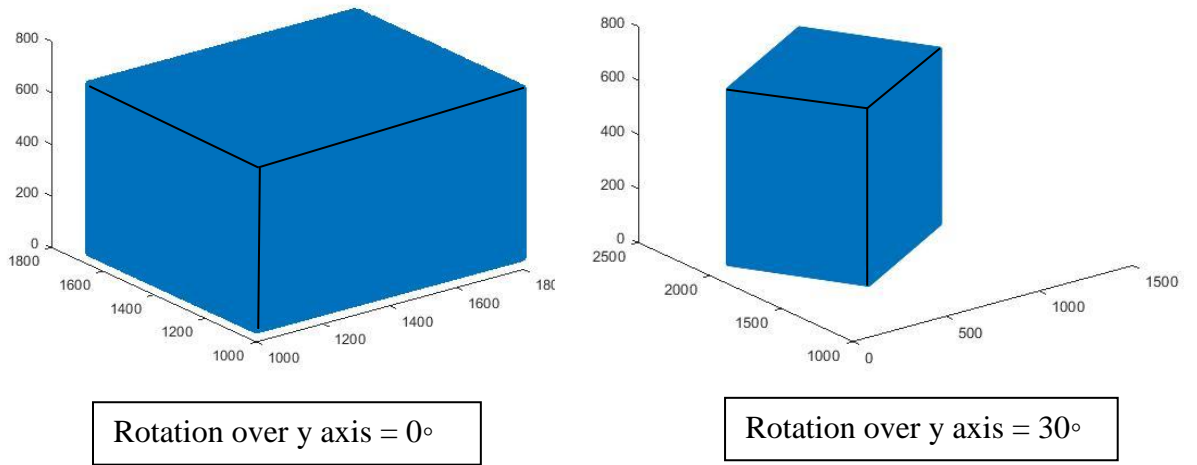


Figure 3-12 : 3-D Model for Rotation over Y Axis

Rotational Metrix R for $k=0$, $\omega = 0$ and $\varphi = 30$.

$$R = \begin{bmatrix} 0.8660 & 0 & 0.5000 \\ 0 & 1.00000 & 0 \\ -0.5000 & 0 & 0.8660 \end{bmatrix}$$

Rotated Point Cloud = $R \times M^T$

2. X-Z plane view of the object

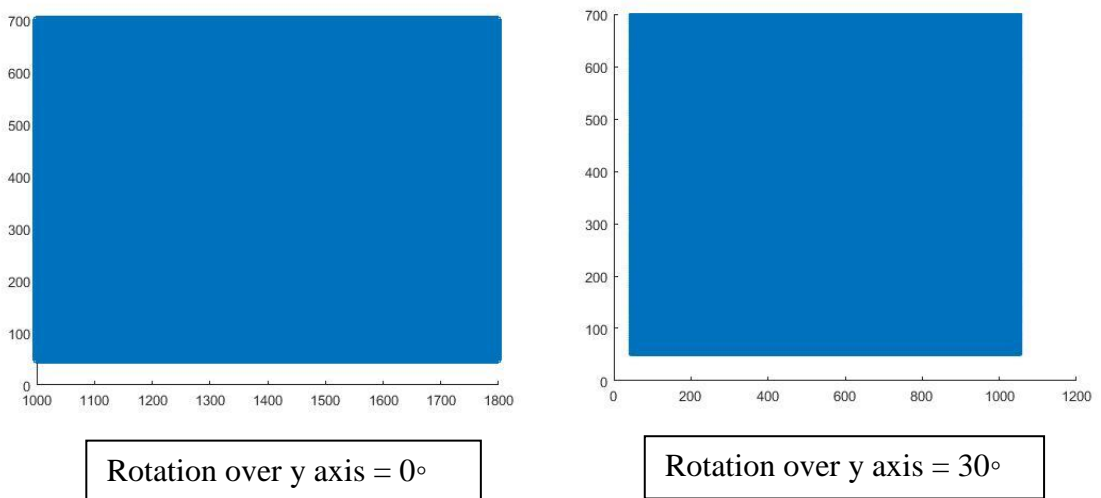
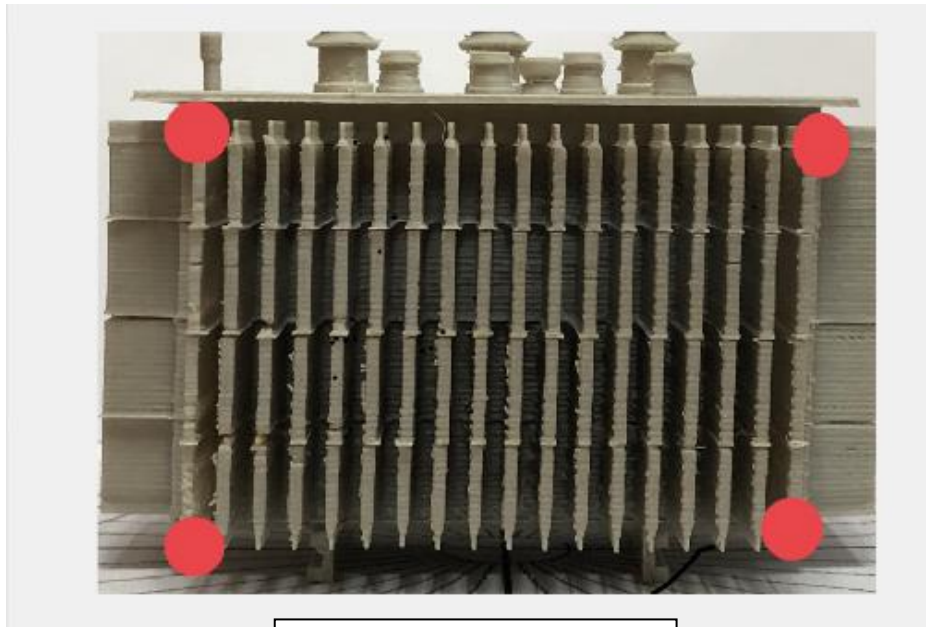


Figure 3-13 : Projection of 3-D Object on X-Z Plane

This projection of the rotated 3D cloud plane is projected X-Z plane as the captured image is in 2-D plane. Superimposing the projection on X-Z plane with the captured image, give the details of the object excluding the background data.

3. *Filtered Image after processing*



Rotation over y axis = 0°



Rotation over y axis = 30°

Figure 3-14: Filtered Image after Processing

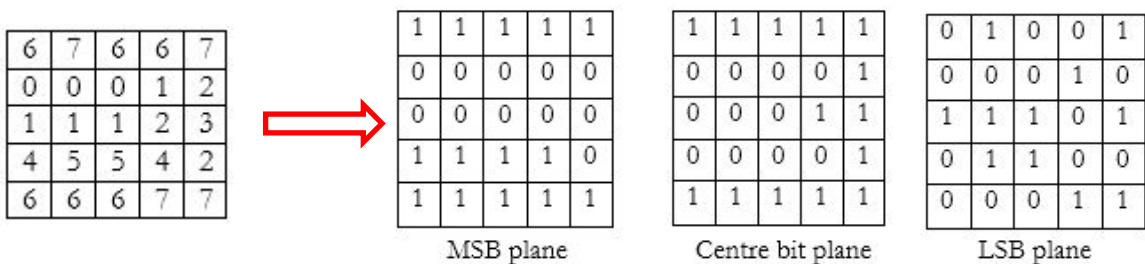
3.1.3 Pattern Recognition

After isolating specific areas of the object as per above steps, the specific visible fault can be located through recognizing pixel patterns. As the first step, the image can be broken down to three planes such as Most Significant Bit Plane (MSB plane), Centre Bit Plane and Least Significant Bit Plane (LSB Plane). Categorizing an image in to these planes can help to easily identify the major pixels which contributes identical color patches in the picture. (Arefin)

Bit plane slicing eliminate noise in the image

$$Bit\ plane_k = Remainder \left\{ \frac{1}{2} floor \left[\frac{1}{2^{k-1}} Image \right] \right\}$$

Slicing is done to identify most significant bit plane and least significant bit planes for analysis.



As an advantage of segregating the image using bit planes, the algorithms can do the analysis faster. Therefore, this methodology can be used to process live streaming data in order to analyze the image on time.

3.1.4 Pattern Clustering

3.1.4.1 Hough transform

The Hough Transform is a dominant tool to find straight lines and functions hidden in pixel clusters. This technique is widely used in image processing as a prominent method to find straight lines. In order to detect lines, the pixels in the image is initially binarized using some thresholding method and then the positive instances catalogued in an examples dataset.

3.1.4.2 Basic Functions

Small radius range is defined for better accuracy.

Range: $r_{max} < 3 * r_{min}$ and $(r_{max} - r_{min}) < 100$.

The accuracy of function increases when the value of radius is larger than 5.

Both computation methods, 'Phase Code' and 'Two Stage' are limited in their ability to detect concentric circles. The results for concentric circles can vary depending on the input image.

Clustering function does not find circles with centers outside the domain of the image. It preprocesses images in binary (logical) patterns to improve the result accuracy. In order to do so, the function automatically convert the true color image to grayscale before processing them.

3.1.4.3 Algorithms

Clustering function uses a Circular Hough Transform (CHT) based algorithm for finding circles in images. This approach is used because of its robustness in the presence of noise, occlusion and varying illumination.

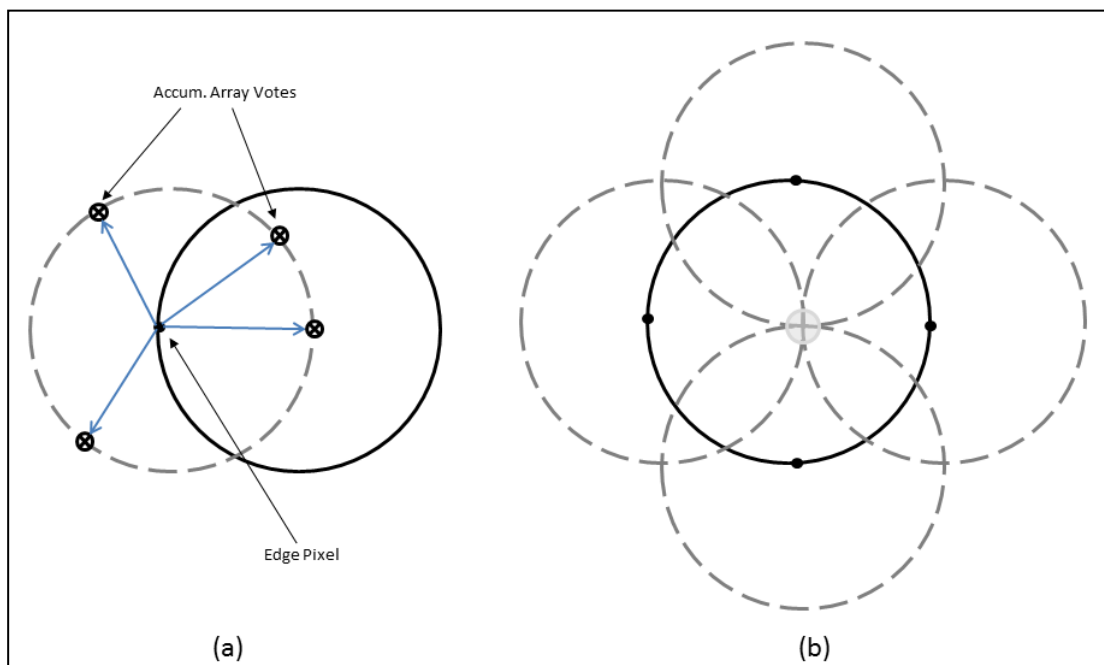


Figure 3-15: Circular Hough Transform

3.1.4.4 Classical CHT Voting Pattern

The pixels belonging to an image circle tend to gather at the accumulator array according to the circle's center. Therefore, the circle centers are predicted by detecting the peaks in the accumulator array.

3.2 Development of the quadcopter

The drone has been designed to inspect energized HV lines and pole top accessories as a remote aerial inspection platform. Due to high magnetizing issues in the MV lines in the distribution networks. This drone is designed to fly stable close to the energized HV power lines by eliminating other stability issues in the commercial drones.

3.2.1 Design Inputs

Lifting capacity: 500g

Flying time: 10 minutes

Maximum speed: 10 ms^{-1}

Size (Approximately): 500mm x 500mm

3.2.2 Design Calculations

The balance of a quadcopter frame is achieved by the adjusting the angular velocities of the rotors which are spun by four electric motors. It has six degree of freedom in both translational and rotational directions which are controlled by those four independent motor signals. In order to achieve such mobility, rotational and translational motion are coupled. The resulting dynamics are highly nonlinear, especially after accounting for the complicated aerodynamic effects. Unlike ground vehicles, quadcopters have very little friction to prevent their motion. Therefore, during the flight, quadcopters must have their own damping in order to stop moving and remain stable.

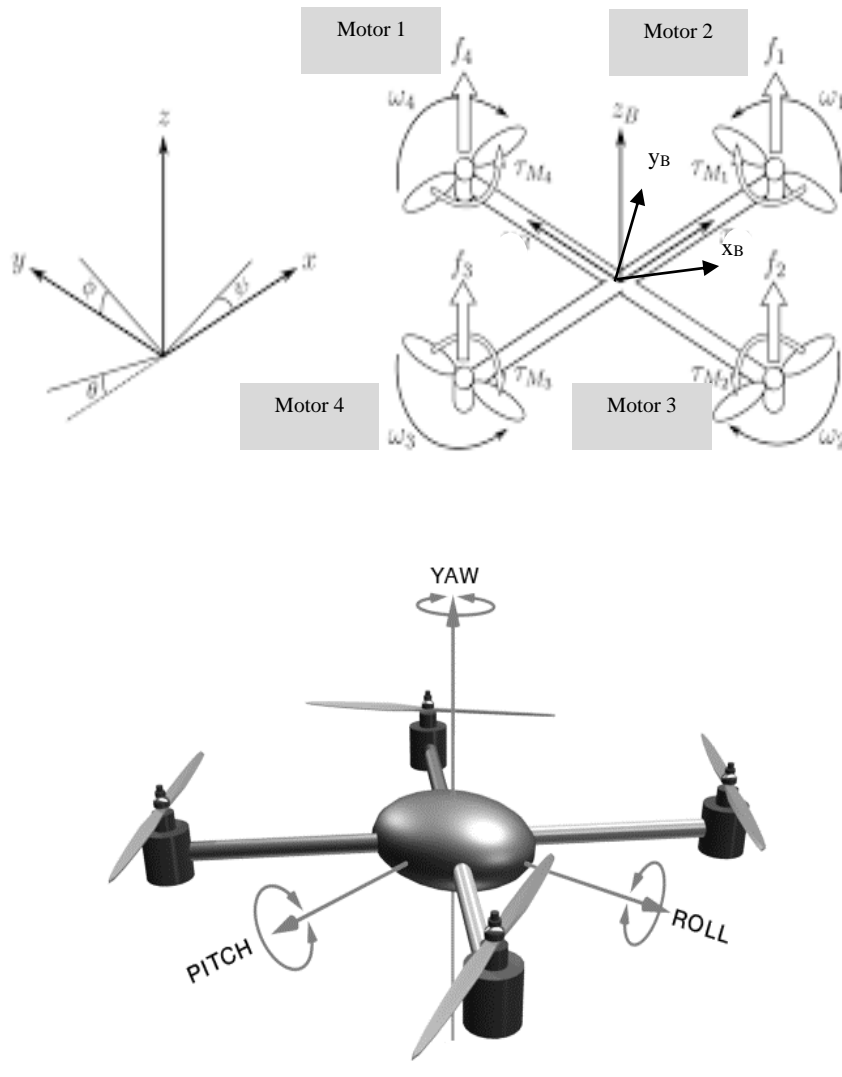
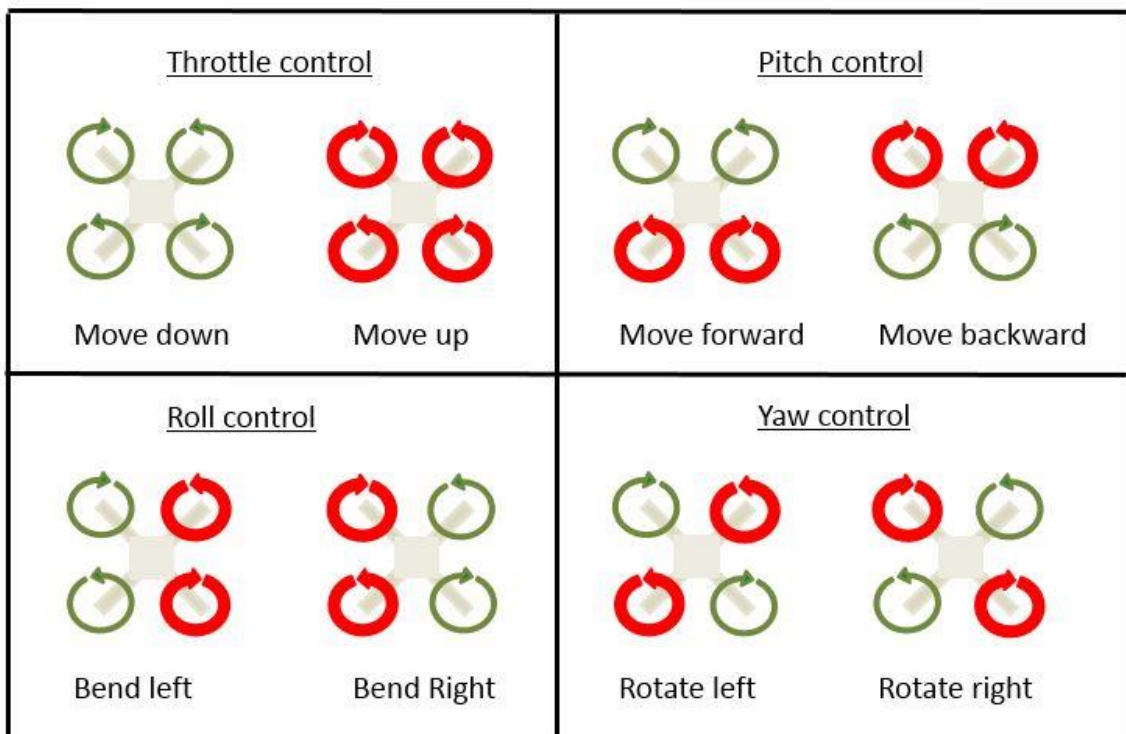


Figure 3-16 : The Inertial and Body Frames of a Quadcopter

When the quadcopter motors spins propellers, it generates a torque which effects on the quadcopter's body in the opposite direction. Hence, if the all motors rotate in the same direction, the resulting force will continuously turn the quadcopter in one direction. In order to counterpart this torque effect, two of the motors are designed to rotate in the opposite direction. Torques are balanced if all propellers are spinning at the same rate. Therefore, the speed difference of the motor pairs which rotate in the same direction will create a resultant torque on the quadcopter body. This mechanism is used to rotate quadcopter in the horizontal plan and this is called yaw of the quadcopter.

The spinning propellers create a thrust on the quadcopter body and when the resultant force ($f_1+f_2+f_3+f_4$) exceed overall weight, it starts moving upwards. This process is used to change the altitude of the quadcopter during the flight and this is called as throttling. While the quadcopter is levelled at the horizontal plan. The resultant force (Z_B) will be parallel to the gravitational force. When the quadcopter is banked at any particular direction, the resultant force (Z_B), will create an additional horizontal force component which will make the frame to drift in that particular direction. This principle is used to move quadcopter forward, backward and side to side which is called pitching and rolling respectively. The entire quadcopter dynamics is achieved by controlling motor pairs in different combinations as in below diagram and the remote controller has four principle servos signals dedicated for this purpose.





-  Normal Speed
-  High Speed

Figure 3-17 : Quadcopter Movements

3.2.3 Kinematics

The position and the velocity of the quadcopter in the inertial frame is considered as $x = (x, y, z)^T$ and $\dot{x} = (\dot{x}, \dot{y}, \dot{z})^T$ respectively. Similarly, the roll, pitch and the yaw angles in the body frames defined as $\theta = (\phi, \theta, \psi)^T$ with corresponding angular velocity equal to $\dot{\theta} = (\dot{\phi}, \dot{\theta}, \dot{\psi})^T$. The vector of the angular velocity (ω) is pointing along the axis of rotation whereas the $\dot{\theta}$ gives the time derivatives of roll, pitch and yaw axis. Therefore, the relationship between can be obtained from trigonometry calculation as follows.

$$\omega = \begin{bmatrix} 1 & 0 & -\sin \theta \\ 0 & \cos \phi & \cos \theta \cdot \sin \phi \\ 0 & -\cos \phi & \cos \theta \cdot \cos \phi \end{bmatrix} \dot{\theta}$$

In order to relate body frame movements in the inertial frame, matrix R can be used which is defined as follows.

$$R = \begin{bmatrix} \cos \phi \cdot \cos \theta - \cos \psi \cdot \sin \phi \cdot \sin \theta & -\cos \phi \cdot \sin \theta - \cos \psi \cdot \cos \theta \cdot \sin \phi & \sin \theta \cdot \sin \phi \\ \cos \theta \cdot \cos \phi \cdot \sin \psi + \cos \psi \cdot \sin \phi & \cos \theta \cdot \cos \phi \cdot \cos \psi - \sin \psi \cdot \sin \phi & -\cos \phi \cdot \sin \theta \\ \sin \phi \cdot \sin \theta & \cos \phi \cdot \sin \theta & \cos \theta \end{bmatrix}$$

Using this conversion matrix, vector \vec{v} in body frame is reflected by $R\vec{v}$ vector in the inertial frame.

3.2.4 Electrical forces (Motors)

The torque (τ) produced in the electric motors is given by

$$\tau = K_t(I - I_0)$$

Where K_t, I and I_0 is denoted by torque proportionality constant, input current and the no load current respectively. The voltage across the motor (V) is sum of the back EMF ($K_v \omega$) and resistive loss (IR_m), where R_m is the motor resistance, K_v is a proportionality constant (back EMF generated per RPM) and ω is angular velocity of the motor.

$$V = IR_m + K_v \omega$$

Therefore, power of the motor (P) is derived from,

$$P = VI = \frac{(\tau + K_t I_0)(K_t I_0 R_m + \tau R_m + K_t K_v \omega)}{K_t^2}$$

Assuming the motor resistance as negligible, power becomes proportional to the angular velocity.

$$P \approx \frac{(\tau + K_t I_0)K_v \omega}{K_t}$$

In practical situations, no load torque is very minimal and therefore, $(\tau + K_t I_0)$ can be assumed as τ .

Hence,

$$P \approx \frac{K_v}{K_t} \tau \omega$$

3.2.5 Aerodynamic Forces

By the law of conservation of energy, the power exerted from the motors is used to keep the quadcopter loitering in the air. The energy that motors spends in a specific time period is the force exerted on the propellers multiplied by the displacement distance of the air it moves.

$$P = F \frac{dx}{dt}$$

Therefore, power is equal to the thrust (T) time air velocity (v_h)

$$P = T v_h$$

At an equilibrium point of the quadcopter in the mid-air, air velocity can be considered as function of thrust as follows,

$$v_h = \sqrt{\frac{T}{2\rho A}}$$

Where, ρ is the density of the surrounding air and A is the area swept by the rotor. Therefore, the power (P) can be simplified as,

$$P = \frac{K_v}{K_t} \tau \omega = \frac{K_v K_\tau}{K_t} T \omega = \frac{T^{\frac{3}{2}}}{\sqrt{2\rho A}}$$

Generally, torque is equal to cross product of force in to the distance vectors, in quadcopter aerodynamic calculations, it is proportional to the thrust. The ratio (K_τ) is determined by the propeller parameters and the blade configuration. The trust is proportional to the square of angular speed.

$$T = \left(\frac{K_v K_\tau \sqrt{2\rho A}}{K_t} \omega \right)^2 = k \omega^2$$

Where, k is a constant. Considering all four motors, the total trust of the quadcopter (on body frame) is derived from;

$$T_B = \sum_{i=1}^4 T_i = k \left[\begin{array}{c} 0 \\ \sum \omega_i^2 \end{array} \right]$$

The additional force on the quadcopter body due to fluid friction is considered as,

$$F_D = \begin{bmatrix} -k_d \dot{x} \\ -k_d \dot{y} \\ -k_d \dot{z} \end{bmatrix}$$

The drag equation from fluid dynamics derives as,

$$F_D = \frac{1}{2} \rho C_D A v^2$$

Whereas, ρ is the surrounding fluid density, C_D is dimensional constant and A is the propeller cross section area. This implies that the torque due to drag (τ_D) is given as a function of C_D , ρ , A, radius of the propeller (R) as follows.

$$\tau_D = \frac{1}{2} R \rho C_D A v^2 = \frac{1}{2} R \rho C_D A (\omega R)^2 = b \omega^2$$

b is defined as some appropriate dimensional constant.

The complete torque about the z axis is the sum of the torque due to drag and the product of moment of inertia (I_M) and angular acceleration ($\dot{\omega}$).

$$\tau_z = b \omega^2 + I_M \dot{\omega}$$

In the steady state flight (with no vertical movement of the quadcopter in mid-air), the propellers are spinning at a nearly constant speed and therefore, torque due to inertial acceleration can be considered as negligible. Therefore, in the steady state flight, the torque about the z axis of the i^{th} motor is derived as,

$$\tau_z = (-1)^{i+1} b \omega_i^2$$

As the half of the motors are spinning in the opposite direction, term $(-1)^{i+1}$ is positive for the i^{th} propeller which is spinning in the clockwise direction and it becomes negative if it is spinning in the counter clockwise direction. Considering all the motors, the total torque (τ_ϕ) on the quadcopter body is given by,

$$\tau_\phi = b(\omega_1^2 - \omega_2^2 + \omega_3^2 - \omega_4^2)$$

The roll and the pitch torques are derived from the same standard mechanism. As shown in the 'Figure 3-17 : Quadcopter Movements', the roll axis movement is identically controlled by motor pairs 1 & 4 and 2 & 3, separately. Therefore, torque on the roll axis

$$\begin{aligned} \tau_\phi &= \sum r \times T = L \left((k\omega_1^2 - k\omega_3^2) + (k\omega_4^2 - k\omega_2^2) \right) \\ &= Lk \left((\omega_1^2 - \omega_3^2) + (\omega_4^2 - \omega_2^2) \right) \end{aligned}$$

Similarly, the torque on the pitch axis can be derived as,

$$\tau_{\theta} = Lk((\omega_1^2 - \omega_3^2) + (\omega_2^2 - \omega_4^2))$$

Where, L is the distance from the center of the quadcopter to any of the propeller. All together, the total torque in the body frame is as follows,

$$\tau_B = \begin{bmatrix} Lk((\omega_1^2 - \omega_3^2) + (\omega_4^2 - \omega_2^2)) \\ Lk((\omega_1^2 - \omega_3^2) + (\omega_2^2 - \omega_4^2)) \\ b(\omega_1^2 - \omega_2^2 + \omega_3^2 - \omega_4^2) \end{bmatrix}$$

3.2.6 Dynamics of the quadcopter

The acceleration of the quadcopter in the inertial frame is based on the trust, gravity and the linear friction of the air drift. Therefore, using rotational matrix R, the liner motion of the quadcopter can be summarized as,

$$m\ddot{\vec{x}} = \begin{bmatrix} 0 \\ 0 \\ -mg \end{bmatrix} + RT_B + F_D$$

Where, \vec{x} is the position of the quadcopter, g is the acceleration due to gravity, F_D is the drag force and T_B is the trust vector in the body frame.

Based on Euler's equation for rigid body dynamics, expressed in vector forms as below,

$$I\dot{\omega} + \omega \times (I\omega) = \tau$$

The angular acceleration vector on quadcopter body frame is mentioned as follows,

$$\dot{\omega} = \begin{bmatrix} \dot{\omega}_x \\ \dot{\omega}_y \\ \dot{\omega}_z \end{bmatrix} = I^{-1}(\tau - \omega \times (I\omega))$$

I is the inertial matrix and τ is a vector of external torques.

Considering the quadcopter body structure, the frame can be considered as four point masses (motors) connected to the corners of two thin uniform rods which are crossed at the center point of each other. Therefore, the inertia matrix I is given by,

$$I = \begin{bmatrix} I_{xx} & 0 & 0 \\ 0 & I_{yy} & 0 \\ 0 & 0 & I_{zz} \end{bmatrix}$$

The final result for the body frame rotational equation of motion is given by,

$$\dot{\omega} = \begin{bmatrix} \tau_{\theta} I_{xx}^{-1} \\ \tau_{\phi} I_{yy}^{-1} \\ \tau_{\psi} I_{zz}^{-1} \end{bmatrix} - \begin{bmatrix} \frac{I_{yy} - I_{zz}}{I_{xx}} \omega_y \omega_z \\ \frac{I_{zz} - I_{xx}}{I_{yy}} \omega_x \omega_z \\ \frac{I_{xx} - I_{yy}}{I_{zz}} \omega_x \omega_y \end{bmatrix}$$

3.2.7 Components used in the design

3.2.7.1 Flight controller

Flight controller usually operates to maintain a reference for the orientations of the quadcopter with respect to the ground during the entire flight time. In fact, the controller should be able to run the equations as mentioned above and control motor speed accordingly at a high frequency. In addition to that, the controller act as the bridge between remote controller and the motors which generates control signal with respect to the user inputs. As the quadcopter responses are very fast, usually flight controller has high speed processors with higher clock speeds in order to process the controlling signal at almost instantly to maintain the precise levels.

3.2.7.2 Gyroscopes and accelerometers

The development of gyroscopes are based upon from mechanical spinning devices which has axles, actuators and gimbals to various materializations of electro- optical devices. Generally multicomputer use “Vibrating Structure Gyroscope” to measure orientations.

Vibrating structure gyroscopes are known as MEMS (Micro-machined Electro-Mechanical Systems) devices which has the ability to operate under Coriolis force

fundamentals. Every point in a rotary system has the same angular velocity. The angular velocity remains constant at the point of axis of rotation of the system whereas the speed decreases along the direction which is perpendicular to the axis of rotation. Therefore, in order to keep the same angular position of the body, it is required to increase or decrease the lateral speed of the system. Hence, the movement should maintain in a straight line in or out from the axis of rotation. During the decreasing or increasing of the speed, the Coriolis force is generated as acceleration times the mass of the object in order to maintain the direction. The Coriolis force proportionally depends on both velocity of the object which is moving in and out from the axis of rotation and the angular velocity.

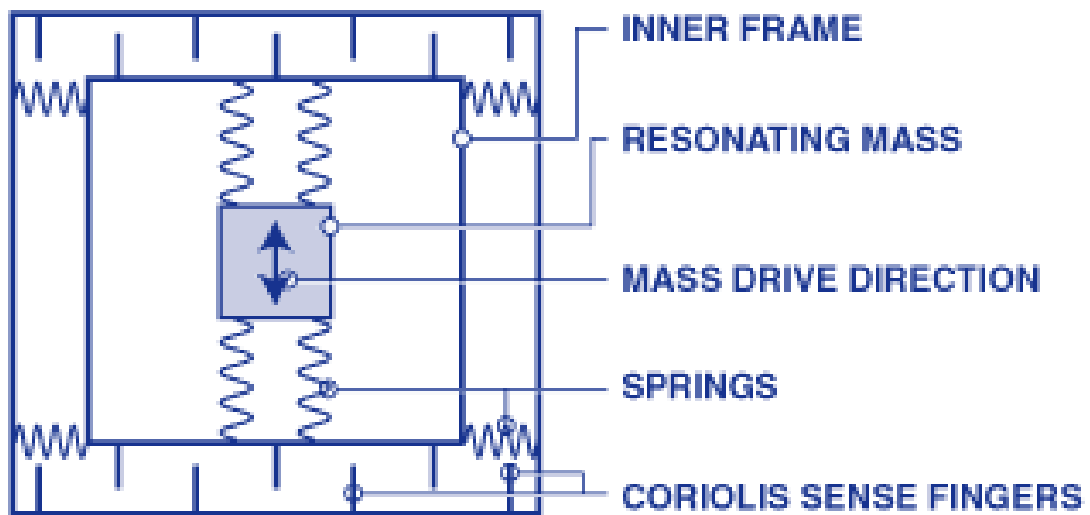


Figure 3-18: Vibrating structure gyroscopes

There is a micro mass inside vibrating structure gyroscopes and it is combined to outer structure by springs. This outer structure also has other orthogonal springs which are connected to the external circuit board. The mass is constantly going through a sinusoidal movement by the first set of springs. The Coriolis acceleration which is induced by rotation of the system, will push the mass towards the direction of the circuit board. The movement of the mass due to Coriolis forces is always perpendicular as it is pushed away from the axis of rotation.

The capacitive sense fingers are used to detect Coriolis that are mounted along the mass housing and the rigid structure. As the mass is moved by the Coriolis force,

sensing fingers are brought closer and differential capacitance will be detected. Therefore, the sensor can recognize both direction and magnitude of the angular velocity of the system.

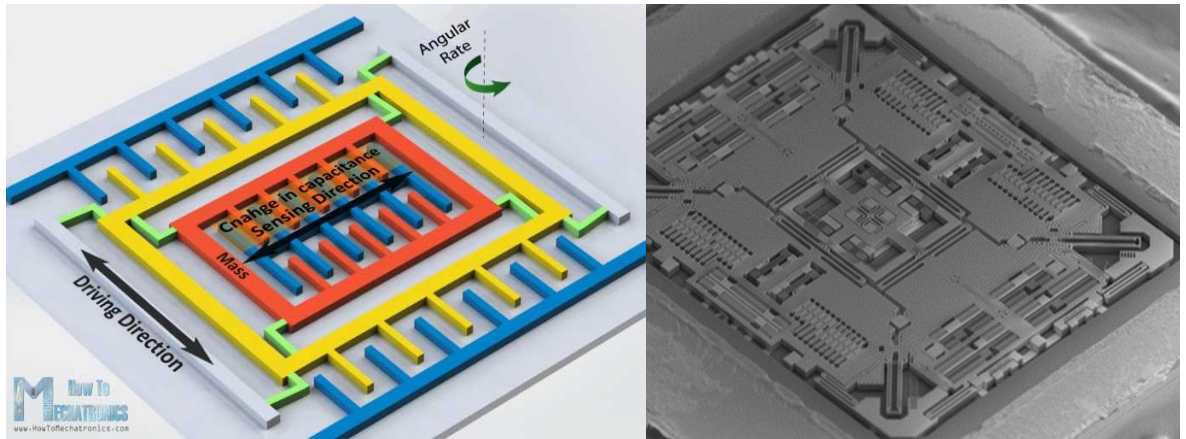


Figure 3-19 : semiconductor wafer architecture (Left) and the real wafer structure (Right) of an Mem Accelerometer

3.2.7.3 Actuators – Brushless DC Motors (BLDC)

Brushless DC motor is a type of electronically commuted motor which do not have brushes. These motors are much efficient in producing large amount of torque at very high speed range. In these kind of motors, there is a permanent magnets rotate around a fixed armature and it avoids the problem of connecting current to the armature. Commutation of the armature is done by power electronics and therefore it has large scope of capabilities and flexibility such as smooth operation, and holding torque when stationary.

Outer Rotor Design

This type of designs has a rotor around the winding which is located in the core of the motor. The heat generated by the motor armature gets trapped inside of the motor due to magnet in the rotor. This motor design operates at low current and has low clogging torque as well.

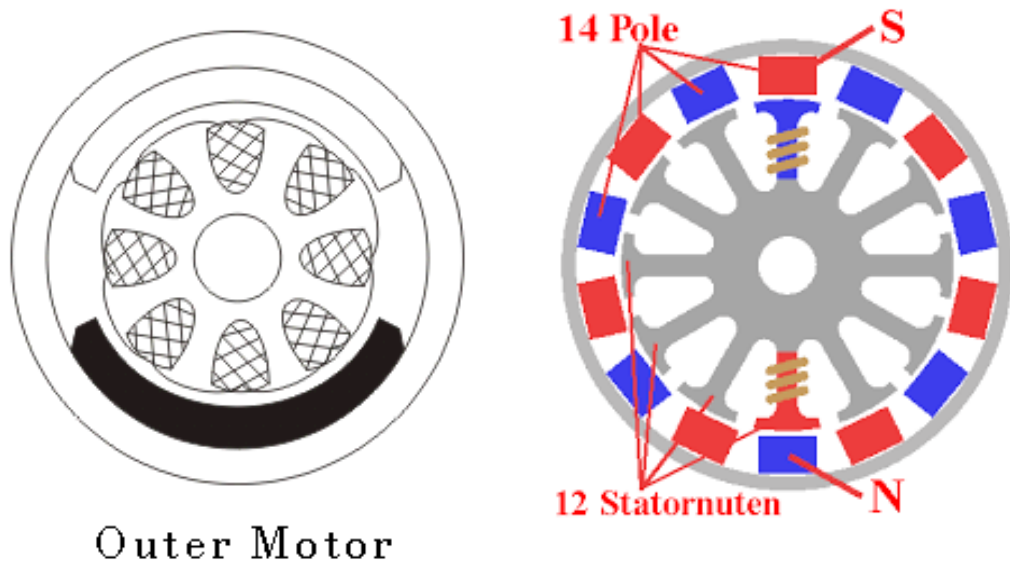


Figure 3-20:Rotor Design

Velocity of BLDC motors is determined by the frequency at which the current is supplied and therefore it is highly efficient in operation. As there are no brushes, mechanical energy loss due to friction is very minimal and it has high lifetime and maintenance free operation. It has no ionizing sparks and therefore electromagnetic interferences are also minimum. Due to low rotor inertia, it can be easily accelerated and decelerated with the control signal.

3.2.7.4 Electronic Speed Controllers

Electronic Speed Controllers (ESC) act as drivers of BLDC motors used in quadcopter and it offers high frequency, high resolution 3-phase AC power to the motors in an extremely compact, lightweight and less space consuming small package. The dynamics of the craft totally depends on varying speed of the motors which drives the propellers. In order to achieve a smooth flight, it is necessary to provide quadcopter propellers a wide RPM variation and fine PWM control.

Generally, quadcopter ESCs can use a higher frequencies compared to the standard 50 Hz signal which is used in other remote controlling appliances. Modern ESC protocols has the ability to communicate higher than 37.5KHz with DSHOT2400 frame. ESC are usually specified according to the operating voltage range and the maximum current it can handle.

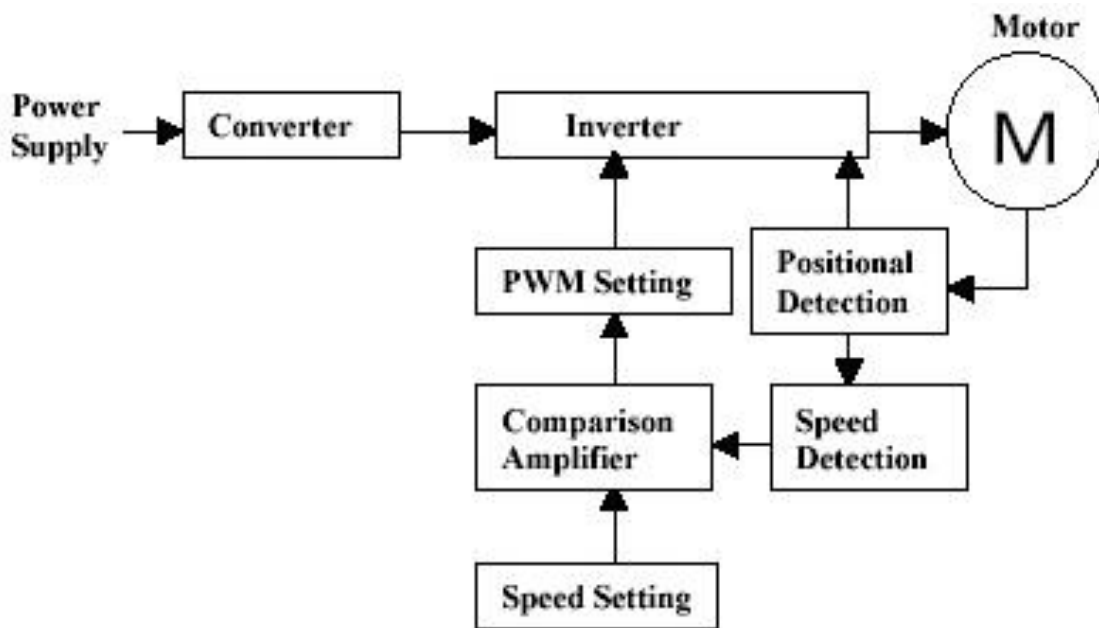


Figure 3-21 : Flow diagram of Speed Controlling Mechanism in ESC

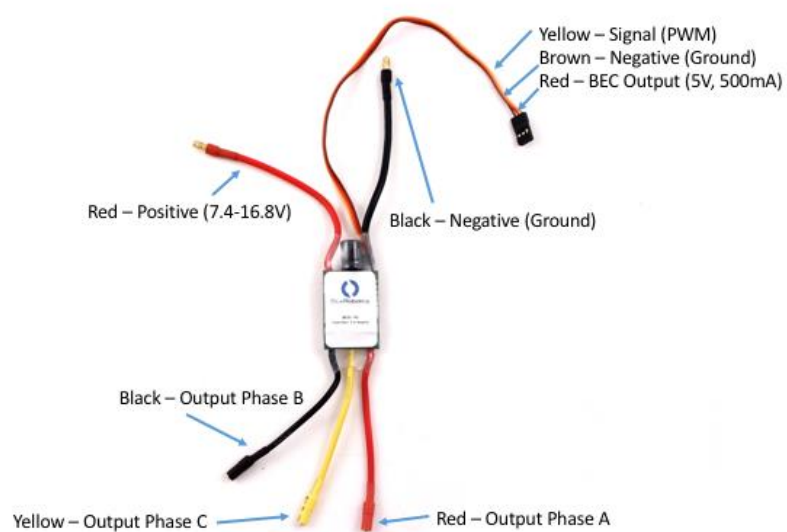


Figure 3-22: General Image of an ESC

3.2.7.5 Radio Transmitter and Receiver

Radio Transmitter generally uses radio signals to send commands over to the receiver through set radio frequency. The transmitter and the receiver should operate in the same set of frequency in order to maintain the communication.

Quadcopter radio transmitter send commands via channels. Each channel carry the instruction for an individual action for the quadcopter. Fundamental commands for quadcopter control such as throttle, yaw, pitch and roll signals has dedicated channels and hence, there should be minimum of four channels to operate the quadcopter. Each channel is allocated to a separate control switch such as slider or knob on the transmitter. The extra channels are used to send the additional information through to the receiver.

Transmitters generally use radio frequencies such as 27MHz, 72MHz, 433MHz, 900MHz, 1.3GHz and 2.4Ghz to communicate with receiver. For long range communications, 433Mhz, 900Mhz and 1.3GHz frequencies are usually used in first-person-view remote controlled systems. Very low frequencies such as 27Mhz and 72Mhz are no longer available in operations.

Nowadays, 2.4GHz is most popular frequency in all most all remote controlling devices. It is a novel technology and it has the ability to do “frequency hopping” which enables to manage transmitting multiple user’s frequency at the same time.. Considering the space constrains of quadcopter design layouts, 2.4GHz is a good fit as the antenna is very small in size.

Some transmitter has the ability to connect external transmitter modules and operate simultaneously. Therefore, it is possible to use a different frequency in the same application with different receiver from another brand/protocol.

Radio communications mainly has two sets of protocols,

- a) TX Protocols between Radio Transmitter and Radio Receiver.
- b) RX Protocols between Radio Receiver and Flight Controller.

Tx protocols are basically depend on the brand or the manufacturer and D8, D16, LR12, DSM, DSM2, DSMX, AFHDS, AFHDS 2A, etc. protocols are commonly

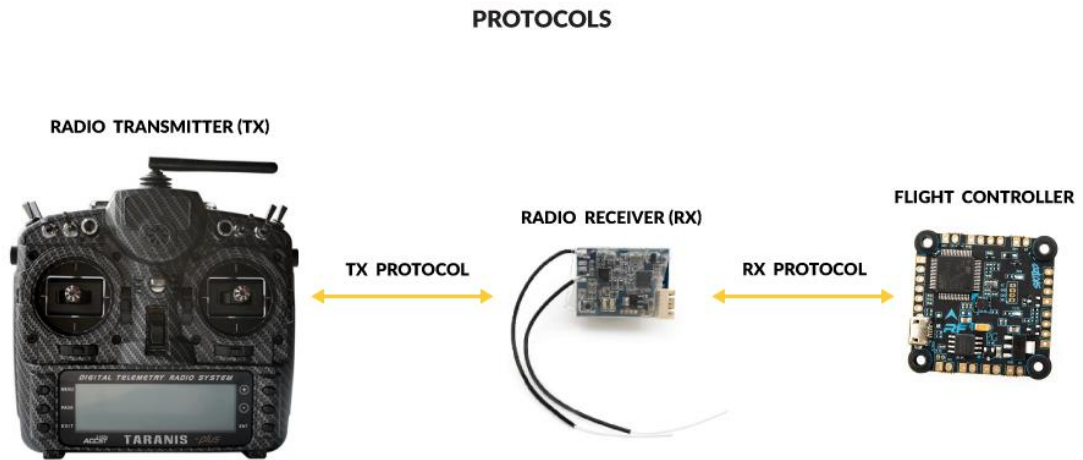


Figure 3-23 : Radio Tx Rx Protocol

used in quadcopters. Generally, receivers has universal protocols but there are brand specified protocols as well. PCM, PWM, PPM, SBUS, iBUS are among these protocols.

3.2.7.6 Power Source - LiPO Battery

Lithium-polymer batteries (LiPos) are commonly used power source for remote guided vehicles such as quadcopters. In this battery type, a lithium-ions from a positive electrode and negative electrode material and therefore it works on the principle of intercalation and de-intercalation of the ion. A liquid electrolyte provides conductive medium for these negative and positive ions. In order to prevent the direct contact of this ions, a microporous separator is placed in between the materials and it allows only the ions to migrate from one side to another while making a barrier for electrode particles.

Lithium-ion cylindrical and prismatic cells have a rigid metal case whereas LiPo cells have a flexible, foil-type (polymer laminate) case. Hence, they are relatively unconstrained. Apparently, cylindrical cells are about 20% heavier than equivalent LiPo cells of the same capacity. Therefore this lightweight provides an advantage for the applications such as quadcopter which requires low weight electronics. However,

the pressure on the stack of layers which make the cells, increases the contacts between the components and thus cell impedance and degradation is maximized. On the other hand, it reduces delamination and deformation of cells. Therefore, the pressure on the stack increases the capacity retention.

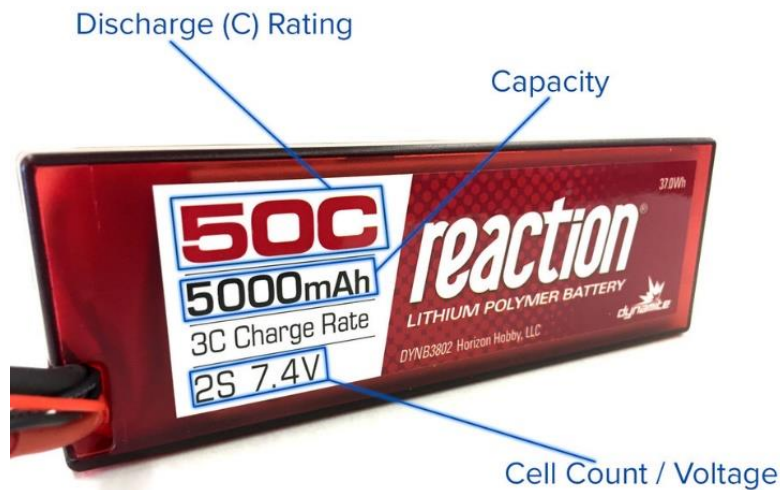


Figure 3-24 : LiPo Battery Rating

Cell Count/ Voltage

A LiPo cell has a nominal voltage of 3.7V. and the formation of cells define the terminal voltage and maximum discharge current of a battery. Number of cells which are connected in series defines the terminal voltage and number of cells which connected in parallel, defines the discharge current. Hence, a two-cell (2S) pack will have an operating voltage of 7.4V and a three-cell (3S) pack will have 11.1V, and so on.

Capacity

The capacity of a battery is basically a measure of how much energy that the battery can provides and the unit of measure here is milliamp hours (mAh). When the rating is high, it provides a long the run time but it increases the weight of the battery pack.

Discharge Rating ("C" Rating)

The 'C' Rating indicates maximum output current of the battery which can be discharged safely and without harming the battery. The maximum discharging rate is calculated using the "C" rating and the battery capacity as follows,

$$50C = 50 \times \text{Capacity (in Amps)}$$

$50 \times 5A = 250A$ Therefore, for above case, the maximum discharging current is . Likewise, for 35C battery which has a 5500mAh capacity, the maximum discharging current will be 192.5A.

3.2.7.7 Ground Station (GCS)

The Ground station unit serves as virtual cockpit for the operator and displays real-time data on the quadcopter performance, position and other important data to operate quadcopter. This application communicates with the quadcopter via wireless telemetry. In advance quadcopter and UAVs, the radio transmitting unit is also embedded with ground stations and therefore it is used to control the vehicle in flight, upload new mission commands and set control parameters as well. It is often also used to monitor the live video streams from a UAV's cameras.

3.2.7.8 Telemetry Unit

Telemetry unit is basically a radio link which help the ground station to communicate with the Quadcopter to exchange data during the flight. Generally, telemetry units have two frequency ranges as 966Mhz and 433Mhz which are used based on the regulations of the country.

4 TESTING AND VALIDATION

Testing procedure was done near to transformer BZ 3079 assembly and 33kV feeder lines which is installed inside the university premises. The transformer is fed by LECO 11kV feeder the assembly has HV components such as DDLOs, Surge arresters, Insulators and strands which is used to mount bare cable to the insulator. In order to identify the flight dynamics near MV distribution lines and line surveying using aerial imaging were tested near 33kV line section inside the university premises.

4.1 Obtaining Close-Up, Zoom Images to Study the Assembly in Details.

Regular inspection process which is done by line patrolling, can only detect the faults and defects by the looks from the ground. But most of the arc flash marks are only visible on the top of insulators. Therefore, those faults can easily be identified using the images taken by the drone. Following images were taken during the test flights and each element can be clearly observed using the remote platform.

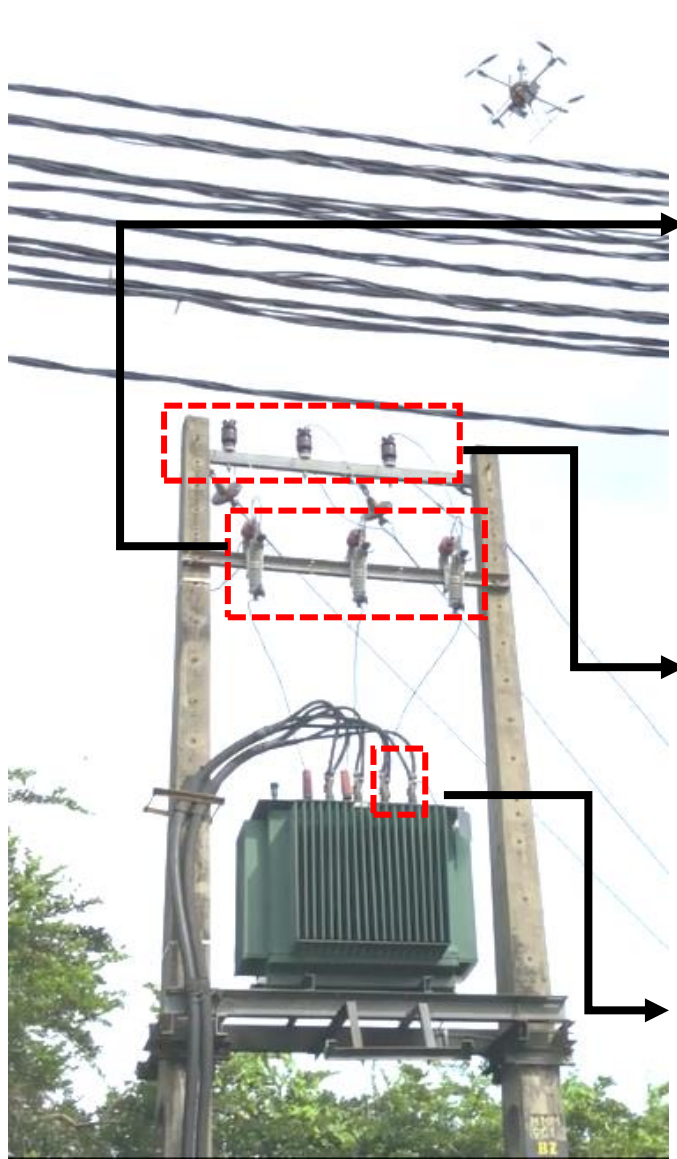


Figure a : DDLO assembly



Figure b : Insulation assembly



Figure c : Transformer LV bushing

Figure 4-1 : Components Inspected Using the Aerial Imaging Platform - BZ3079 Transformer

4.1.1 Insulation Assembly

Damages due to arc flashes create insulation failures and the line get tripped due to the operation of earth fault relays in downstream. In order to restore the power system, it is mandatory to identify the faulty insulator due to arc flash. From line patrolling, it is difficult to locate arc flash marks on insulator tops from ground level and therefore efficiency of clearing fault is related to this issue is very low. Hence, using information from the precise, aerial images can improve the efficiency of identification of insulation faults.

On the other hand, from the level of details available in the image, the status of the cable ties and preforms can be identified. This feature is also a major advantage of inspection through aerial images vs conventional line patrolling method.

4.1.2 DDLO and Surge Arrester Assembly

Earth link for surge arrestors is extremely important in order to protect equipment from surges. Poor connection, broken conductors of earth links can create high impedances for short circuit path and therefore, it will damage the downstream assets such as transformers and consumer goods. Clear information about the status of the earth link connections can be taken from aerial images and therefore the accuracy of the inspection is high.

4.1.3 Transformer LV Bushing

Owing to the construction of a typical transformer, LV bushings are short in size and it's hardly visible to the ground when it is mounted on top of the pole. Therefore, during general line inspection, the status of this barely seen. As LV terminals carry high current, poor connection in the flag to lug terminals can cause not only fire hazards due to temperature rise but power losses in distribution systems. Through aerial imaging the status of the terminals such as corroded nuts and bolts, broken lugs, oil leak marks on transformer top can be clearly investigated. Therefore, information which is gathered from aerial imaging is more important to schedule planned maintenance effectively.



Figure 4-2 : View of the Transformer Assembly from Ground



Figure 4-3 : Detailed View of the Transformer Assembly from Aerial Imaging

4.2 Feeder Line Surveying

Prior to HV feeder line rehabilitation project, it is a mandatory requirement to perform a survey to identify the existing arrangement of the feeder. This information is used in the planning stage to identify the obstacles and limitations in order to optimize the construction process. In the current situation, online services such as Google street maps, Google earth are

used to do this survey. But, aerial imaging provides more accurate and real-time details about the situation and hence, it can be used to do the survey effectively. Even though, using aerial imaging for survey purposes doesn't directly impact reducing system outages, it adds more values to the operation by giving ability to dynamically observe feeder arrangement in gantry points, vegetation level, line overlapping and type of the pole used in construction.





Figure 4-4 : Line Surveying - 33kV Feeder Section in UoM

4.3 Image Patch and Defect Identification Algorithm Testing

As discussed in previous chapter, processing of the images can be done subjected to the visual demarcations of the equipment boundaries. In the current contest, there are no any demarcation in the existing MV lines, the algorithm was tested for a known item, i.e. the transformer assembly in BZ3079 unit. The accuracy of the algorithm was tested to identify the corroded nuts and bolts in transformer LV terminals.

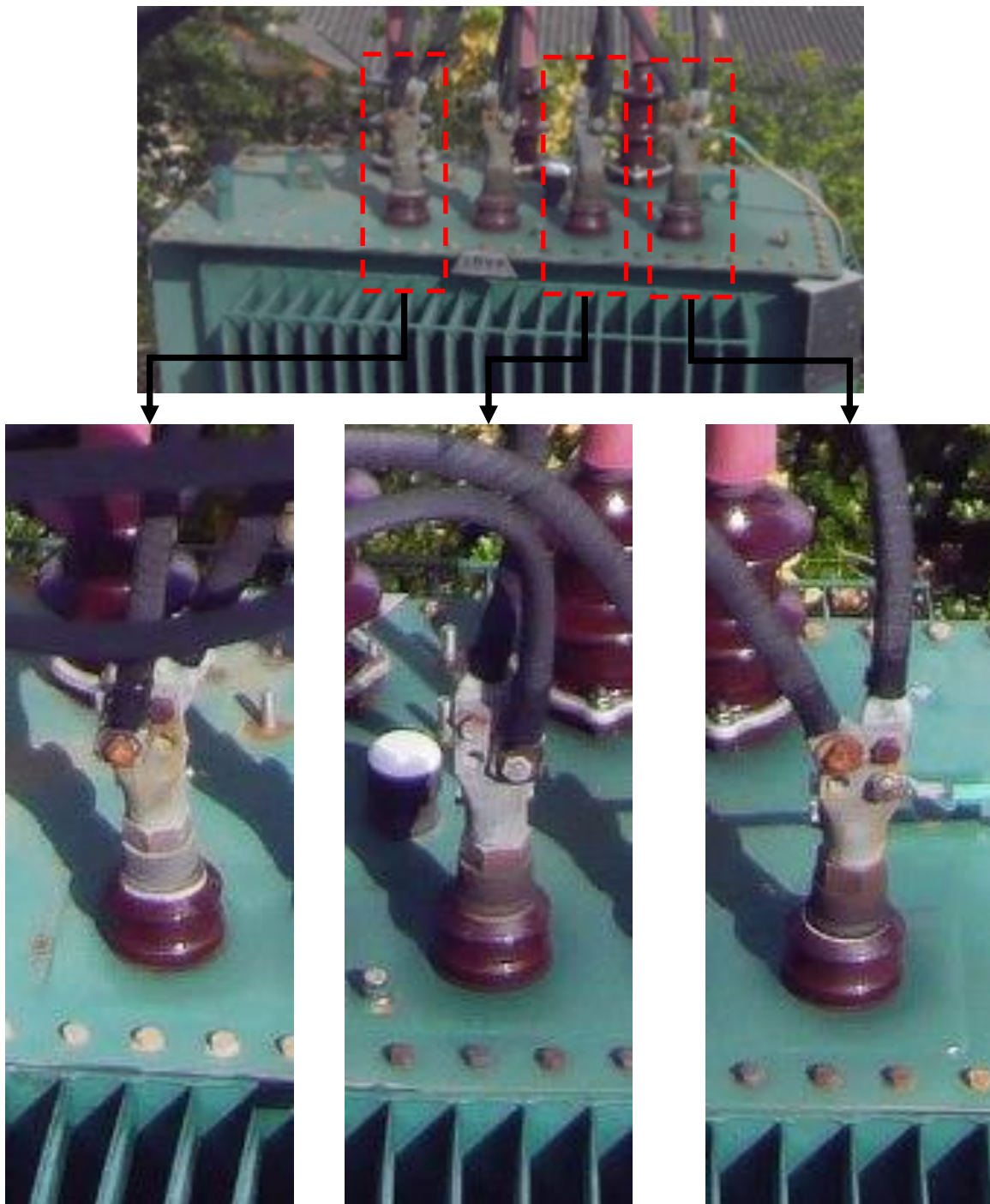


Figure 4-5 : Identification of Focus Area to be Processed

Dimension ratio in the transformer is used to identify each LV terminal

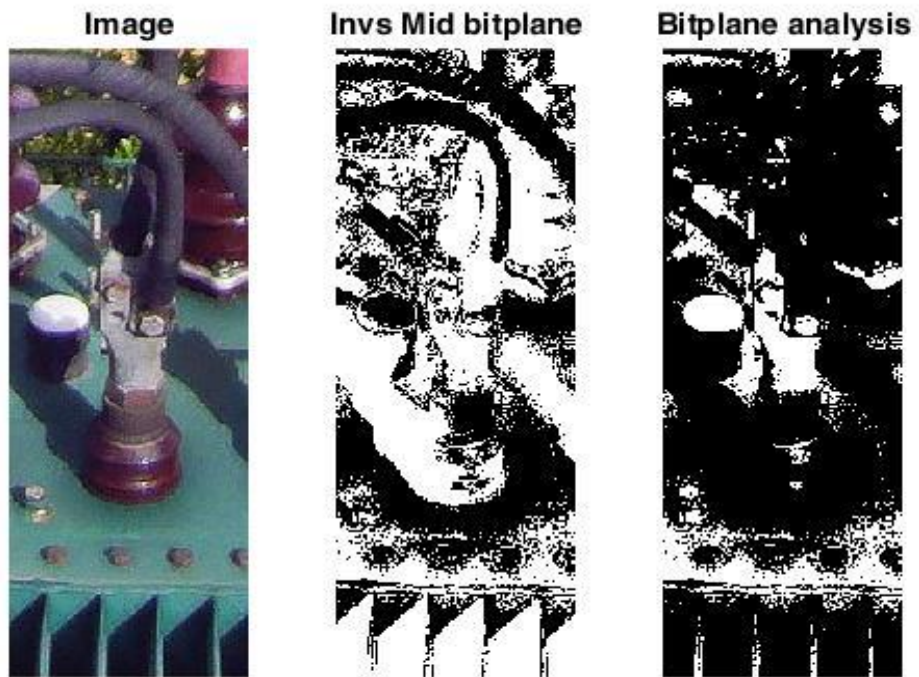


Image 1

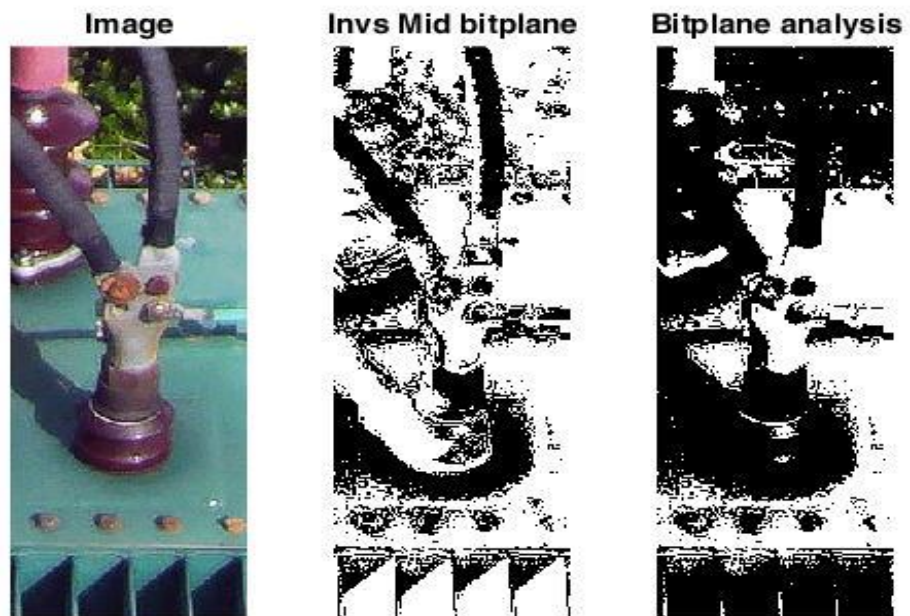


Image 2

Figure 4-6 : Bit Plane Slicing Algorithm for LV Terminal







Applying bit plane slicing algorithm to identified LV terminal image section

The Most significant bit plane was used to identify the corroded color patches on the terminals. Comparison was done between original image and MSB plane in order to identify the accuracy of algorithm in both conditions.

Table 4-1 : Parameters Used to Identify Corroded Nuts and Bolts

	Nuts in good condition	Nuts in bad condition
Radius (Minimum) / Pixel	10	200
Radius (Maximum) / Pixel	20	250
Sensitivity	91%	97%

Table 4-2 : Summary of Color Patch Detecting Algorithm Testing

	Case 1 – Raw Image	Case 1 – Processed Image	Case 2 – Raw Image	Case 2 – Processed Image	Case 3 – Raw Image	Case 3 – Processed Image
Sample Images						
Number of Correct detections	-	0	0	1	0	1
Number of Incorrect Detections	3	0	5	0	3	0
Number of non -detections	1	1	1	1	2	1

The results reveal that the algorithm reduce number of incorrect detections. Even though this is not the absolute solution to fully automate the fault identification and un-man process, this can be used to filter most significant images with defects for further inspection. As like in many other object recognition algorithms, it helps to increase the accuracy of inspection process by highlighting areas for operator’s attention without wasting much time to evaluate the entire image.

4.4 Quadcopter Testing

4.4.1 Tuning the Parameters

The algorithm uses PID control loop mechanism to achieve precise outputs of each motor with respective to the controlling signal. The parameters of the initial designed was determined as follows in order to obtain smooth controlling of the drone

Table 4-3 : PID values used in Quadcopter

Parameter	Rolling axis	Pitching axis	Yaw axis
P :	0.153222	0.17473	1.0480
I :	0.153222	0.17473	0.1048
D :	0.006211	0.006833	0.0000

4.4.1.1 Control Signal Vs Drone Response with Initial Parameters



Figure 4-7 : Before Tuning the PID Parameters in Pitch Axis – Badly Aligned Controlling Signal and Response

4.4.1.2 Control Signal Vs Drone Response After Applying the Current Parameters

The alignment of controlling signal and the response is also overlapped for the roll and yaw axis for above mentioned PID values.

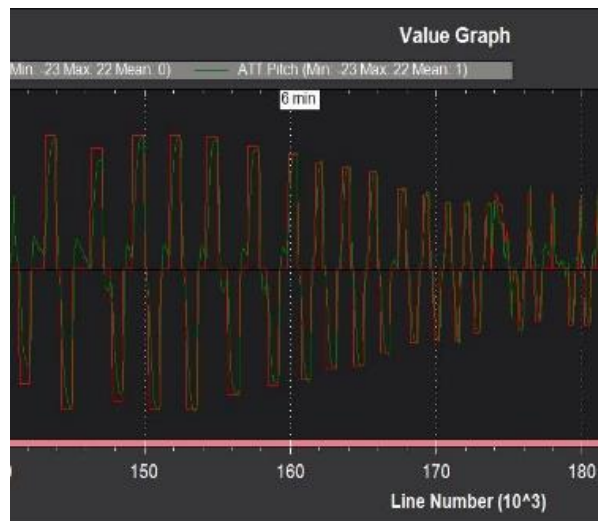
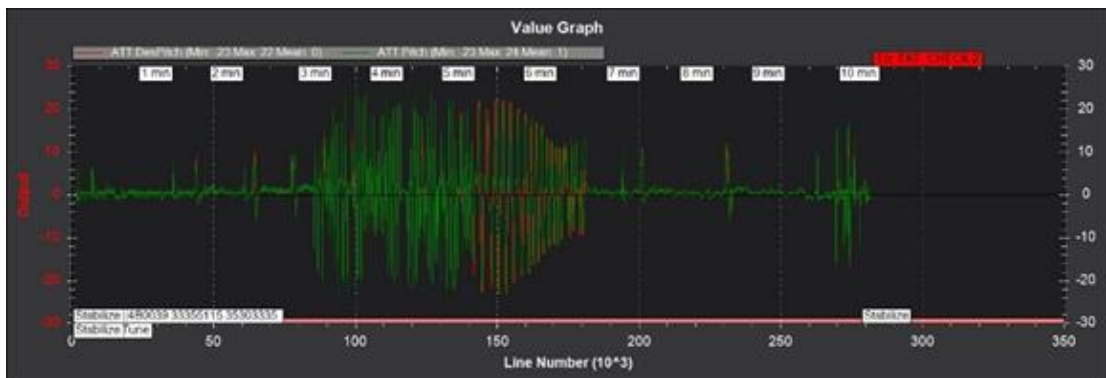


Figure 4-8 : After Tuning PID Values in Pitch Axis - Controlling Signal and Response is Substantially Overlapped

Due to the high power consumption of additional stability equipment such as LiDAR range finder and flow sensor, the actual flying time of the drone was dropped to approximately about 4 minutes and therefore, the second drone was designed to overcome the challenges.

With proposed configuration as per the drone design, the optimum speed of the drone is 24km/h and the expected flight time is 5.5 mins with the payload. This delivers maximum flight distance of 2000m and therefore the drone can be operated within 1 km span considering the total back and forth travelling distance. Imaging unit can capture 30 frames per second and therefore, in this operational state, 6 images can be taken per 1 meter of distribution line. This image rate is satisfactory for obtain relevant information on a feeder line.

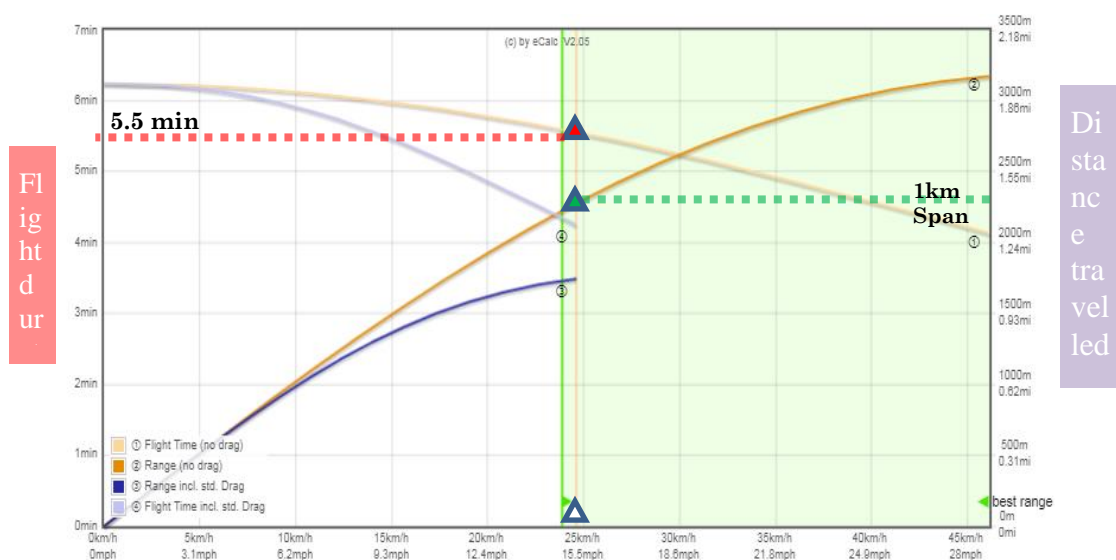


Figure 4-9 : Flight Characteristics of Quadcopter

4.4.2 Altitude Holding Function

As the flight controller get barometer reading from two sensors, better altitude holding was achieved for the new design. Therefore, the maneuvering has become easy for the new drone when flying the “Altitude Hold” mode.

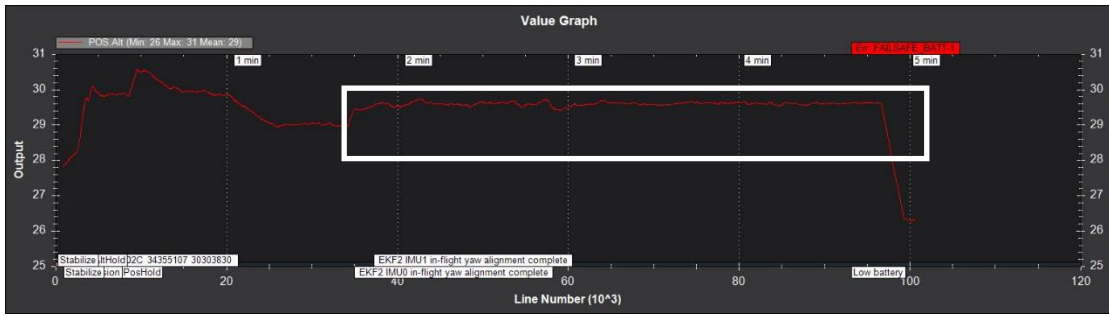


Figure 4-10 : Altitude is Remain Constant in the "Altitude Hold" Mode

4.4.3 Impact Analysis on Time and Space Requirement for Inspection Process

Table 4-4 : Impact Analysis on Time and Space Requirement for Inspection Process

	Line Patrolling with ladders			Bucket Truck Deployment			Aerial Observation Platform		
	Time (min)	Space (m ²)	Network outage Time (min)	Time (min)	Space (m ²)	Network outage Time (min)	Time (min)	Space (m ²)	Network outage Time (min)
Transformer Inspection	60	2	20	30	20	10	5	2	0
Line Inspection (500m span)	180	20	180	50	80	0	10	2	0
Insulator Inspection	30	2	30	15	15	0	3	2	0

4.5 Limitation of the Study

The design of the aerial platform was done to build the hardware within a limited budget. Therefore, the design of the aerial platform was done to build the hardware to run algorithms and check the usability in the practical environment.

The existing MV lines doesn't have visual demarcations for equipment boundaries and therefore image processing algorithm was tested only for one known equipment;

i.e., the transformer assembly in BZ3079 substation. Should the utility use this algorithm for fault identification process, the equipment in the lines shall be demarcated as per the design and algorithm has to be customized to for each type of fault.

Image processing and analysis algorithms were developed in MATLAB platform in order to identify the accuracy of the results. Hence, real-time processing for an incoming video stream is not possible with selected software platform. The finalized algorithm can be transformed to portable software platforms such as python or Open MV, in order to facilitate processing live video feeds.

5 CONCLUSION

The energy need of urban community in Sri Lanka is highly dependent on the electricity supply. This consumer behavior and its impact on Sri Lankan economy, the regulatory body is drastically pushing utilities reduce outage time. Now, it has come to a stage where a compensation system has been proposed for consumers who undergo more system outages than the nominal level while imposing penalties to utilities.

Mainly the outages are occurred due to system maintenance and it's considered as an essential element in the operation of distribution system. The maintenance process includes several steps and among those, inspection is considering as a necessary but non-value adding activity which cannot be compromised. Considering the advanced technologies used in other industries, there are opportunities to improve the efficiency of this inspection process which apparently reduce the outage time and increase system reliability.

In this study, concept of having a remote aerial platform with a camera unit is introduced. As the method of inspection, camera unit and image processing is proposed and as the aerial platform, the design and the development of a quadcopter is proposed. The design has the capability to capture and process images to identify basic faults and run across the HV lines while mitigating electromagnetic interferences.

Case study comparison proves that inspection process through the proposed system brings more advantages over conventional, manual inspection process. The ability takes images in 360° scope of view itself bring lot of benefits over limited eye inspection from ground. Remote operation of the camera unit increases the safety of inception procedure as it minimizes human involvement closer to HV lines. Further, automated fault identification algorithm improves probability of detecting images with defects and hence, it improves the efficiency of the process.

Depending on the operational requirement such as span of inspection, time of inspection and nature of the investigation, the design parameters can be selected to increase the flight time, duration and camera resolution accordingly. Therefore, this concept can be customized to utilize to improve efficiency and quality of any overhead MV line inspection activity in urban areas in Sri Lanka.

6 REFERENCES

1. Liyan Zhang, Shouyin He, “Mobile Robot for Overhead Powerline Inspection and a controlling method for obstacle avoidance” in 2011 International Conference on Electric Information and Control Engineering.
2. A. Pagnano, M. Höpf, R. Teti, “A roadmap for automated power line inspection, Maintenance and repair” in 8th CIRP Conference on Intelligent Computation in Manufacturing Engineering
3. C. Huang Shen, F. Y. C. Albert, C. K. Ang and Dwee Jin Teck, “Theoretical development and study of takeoff constraint thrust equation for a drone” in 2017 IEEE 15th Student Conference on Research and Development.
4. Edgar A. Niit, Willie J. Smit, “Integration of Model Reference Adaptive Control (MRAC) with PX4 Firmware for Quadcopters” 2017 24th International Conference on Mechatronics and Machine Vision in Practice (M2VIP)
5. Donggyun Kim, Jinho Park, Junghoon Jung, Taechan Kim and Joonki Paik, “Lens Distortion Correction and Enhancement Based on Local Self-similarity for High-quality Consumer Imaging Systems” in IEEE Transactions on Consumer Electronics (Volume: 60, Issue: 1 , February 2014).
6. Edgar A. Niit, Willie J. Smit, “VTOL aerial Robot for inspection of Transmission line” 2017 24th International Conference on Mechatronics and Machine Vision in Practice (M2VIP)